Viability Control for a Class of Underactuated Systems

Dimitra Panagou [a], Kostas J. Kyriakopoulos [a]

[a] *Control Systems Lab, School of Mechanical Engineering, National Technical University of Athens, Greece*

Abstract

This paper addresses the feedback control design for a class of nonholonomic systems which are subject to inequality state constraints defining a constrained (viability) set K. Based on concepts from viability theory, the necessary conditions for selecting viable controls for a nonholonomic system are given, so that system trajectories starting in K always remain in K. Furthermore, a class of state feedback control solutions for nonholonomic systems are redesigned by means of switching control, so that system trajectories starting in K converge to a goal set G in K, without ever leaving K. The proposed approach can be applied in various problems, whose objective can be recast as controlling a nonholonomic system so that the resulting trajectories remain for ever in a subset K of the state space, until they converge into a goal (target) set G in K. The motion control for an underactuated marine vehicle in a constrained configuration set K is treated as a case study; the set K essentially describes the limited sensing area of a vision-based sensor system, and viable control laws which establish convergence to a goal set G in K are constructed. The robustness of the proposed control approach under a class of bounded external perturbations is also considered. The efficacy of the methodology is demonstrated through simulation results.

Key words: Constraint Satisfaction Problems, Constrained Control, Underactuated Robots, Nonholonomic Control, Robot Control, Convergent Control, Invariance, Disturbance rejection, Robust control.

1 Introduction

Nonholonomic control has been and still remains a highly challenging and attractive problem from a theoretical viewpoint. Related research during the past two decades has attributed various control design methodologies addressing stabilization, path following and trajectory tracking problems for nonholonomic systems of different types, which nowadays feature a solid framework within control theory.

From a practical viewpoint, nonholonomic control is of particular interest within the fields of robotics and multi-agent systems, since a significant class of robotic systems is subject to nonholonomic constraints. The control design in this case typically pertains to realistic, complex systems, which should perform efficiently and reliably; in this sense, the robustness of control solutions with respect to (w.r.t.) uncertainty and additive disturbances is a desirable property, which highly affects the performance, or even safety, of the considered systems. In part for this reason, the development of robust nonholonomic controls w.r.t. vanishing, as well as non-vanishing perturbations has received special attention, see [1–10] and the references therein. Non-vanishing perturbations are typically more challenging, since a single desired configuration might no longer be an equilibrium for the system [11]. In this case one should rather pursuit the ultimate boundedness of state trajectories; this problem is often addressed as practical stabilization. In a similar context, the development of input-to-state stability (ISS) as a fundamental concept of modern nonlinear feedback analysis and design, has allowed the formulation of robustness considerations for nonholonomic systems into the ISS framework [12–15].

Furthermore, one often can not neglect that control systems are subject to hard state constraints, encoding safety or performance criteria. An illustrative paradigm of hard state constraints is encountered in the case of agents that have limited sensing capabilities while accomplishing a task. For instance, consider an underactuated robotic vehicle equipped with sensors (e.g. cameras) with limited range and angle-of-view, which has to surveil a target of interest; the requirement of always having the target in the camera field-of-view (f.o.v.) imposes a set of inequality state constraints, which should never be violated so that the target is always visible. This problem, often termed as maintaining visibility, applies in leader-follower formations where the leader is required to always be visible to the follower [16–19], in landmark-based navigation [20–22], in visual servo control [23, 24], or in visibility-based pursuit-evade prob-

⋆ This paper was not presented at any IFAC meeting. Corresponding author Dimitra Panagou. Tel. +30-210-772-3656.

Email addresses: dpanagou@mail.ntua.gr (Dimitra Panagou), kkyria@mail.ntua.gr (Kostas J. Kyriakopoulos).

lems, see [25] and the references therein. Similar specifications in terms of state constraints apply in maintaining connectivity problems, involving n nonholonomic agents with limited sensing and/or communication capabilities that have to accomplish a common task while always staying connected [26].

1.1 Contributions

This paper proposes a control design methodology for a class of nonholonomic systems which are subject to hard state constraints. The state constraints are realized as nonlinear inequalities w.r.t. the state variables, which constitute a closed subset K of the state space $\mathcal{Q}$. The set K is thus the subset of state space in which the system trajectories should evolve $\forall t \geq 0$. System trajectories which either start out of K, or escape K for some $t > 0$ immediately violate the state constraints and thus are not acceptable. Therefore, the control objective reduces into finding a (possibly switching) state feedback control law, so that system trajectories starting in K converge to a goal set G in K without ever leaving K.
The proposed approach combines concepts from viability theory [27] and results from our earlier work on the state feedback control of n-dimensional nonholonomic systems with Pfaffian constraints [28] (Section 2). In the sequel, following [27], state constraints are called viability constraints, the set K is called the viability set of the system, and system trajectories that remain in K $\forall t \geq 0$ are called viable (Section 3). In particular, we adopt the concept of tangency to a set K defined by inequality constraints [27], and provide the necessary conditions under which the admissible velocities of a kinematic nonholonomic system are viable in K, as well as the necessary conditions for selecting viable controls (Section 4). In addition, given the control solutions in [28], we propose a way of redesigning them by means of switching control, so that the resulting trajectories are viable in K and furthermore converge to a goal set $G \subset K$. As a case study, we consider the motion planning for an underactuated marine vehicle which is subject to configuration constraints because of limited sensing (Section 5); the onboard sensor system consists of a camera with limited angle-of-view and two laser pointers of limited range. The task is defined as to control the vehicle so that it converges to a desired configuration w.r.t. a target of interest, while the target is always visible in the camera f.o.v.; in that sense, this is also a problem of maintaining visibility. The visibility maintenance requirement, along with limited sensing, impose a set of configuration constraints that define a viability set K. The robustness of the proposed control approach under a class of bounded perturbations is studied in Section 6. Our conclusions and plans for future extensions are summarized in Section 7.
The problem formulation is similar to the characterization of viable capture basins of a target set C in a constrained set K [29], which is based on the Frankowska method that characterizes the backward invariance and (local) forward viability of subsets by means of the value function of an optimal control problem. However, in this paper we rather address the problem in terms of set invariance [30, 31], where the objective is to render the viability set K a positively invariant (or controlled invariant) set, and the goal set G the largest invariant set of the system by means of state feedback control. [1]
The notion of controlled invariance for linear systems has been utilized for the control design of systems with first-order (kinematic) nonholonomic constraints, after linearizing the nonlinear system equations around the equilibrium [18]; compared to this work, here we present a method which addresses a wider class of constrained underactuated systems, including the class of nonholonomic systems with second-order (dynamic) nonholonomic constraints, without the need for linearizing the system equations.
The motion control of underactuated marine (underwater, surface) vehicles and ships has been treated in the past using various control design techniques, see for instance [32–38] and the references therein; however, to the best of our knowledge, none of the relevant work considers any additional state (configuration) constraints on the system. Furthermore, in this paper we present a novel motion control scheme for the considered class of underactuated marine vehicles, based on our methodology for the state feedback control for n-dimensional nonholonomic systems [28].
In relation to our prior work in [39], here we do not adopt an optimal control formulation, and propose control solutions that not only remain in K, but also converge to a goal set $G \subset K$. Compared to [40], we consider a wider class of viability constraints, while we further address the viable robust control design of underactuated systems w.r.t. a class of bounded external perturbations.

1.2 Overview

We consider the class of nonlinear systems described by

$$\dot{\boldsymbol{q}} = \boldsymbol{f}(\boldsymbol{q}, \boldsymbol{u}), \quad \boldsymbol{u} \in \boldsymbol{U}(\boldsymbol{q}), \tag{1}$$

where $\boldsymbol{q} \in \mathcal{Q}$ is the state vector, $\mathcal{Q} \subset \mathbb{R}^n$ is the state space (a normed space), $\boldsymbol{u} \in \mathcal{U}$ is the vector of $m < n$ control inputs, $\mathcal{U} \subset \mathbb{R}^m$ is the control space, $\boldsymbol{U} : \mathcal{Q} \rightsquigarrow \mathcal{U}$ is a feedback set-valued map associating with any state $\boldsymbol{q}$ the (possibly empty) subset $\boldsymbol{U}(\boldsymbol{q})$ of feasible controls at $\boldsymbol{q}$ and $\boldsymbol{f} : \mathrm{Graph}(\boldsymbol{U}) \mapsto \mathcal{Q}$ is a continuous single-valued map, which assigns to each state-control pair $(\boldsymbol{q}, \boldsymbol{u}) \in \mathrm{Graph}(\boldsymbol{U})$ the velocity $\boldsymbol{f}(\boldsymbol{q}, \boldsymbol{u})$ of the state, i.e. the (tangent) vector $\dot{\boldsymbol{q}} \in \mathcal{Q}$.
The system (1) is subject to $\kappa < n$ nonholonomic constraint equations. [2] Each constraint $i \in \{1, \ldots, \kappa\}$ is

[1] The viability property has been introduced as "controlled invariance" for linear and smooth nonlinear systems [27].

[2] Typically, *kinematic* nonholonomic constraints can be written in Pfaffian form as $\boldsymbol{A}(\boldsymbol{q})\dot{\boldsymbol{q}} = \boldsymbol{b}(\boldsymbol{q})$, where $\boldsymbol{q} \in \mathbb{R}^n$ is the vector of generalized coordinates, $\boldsymbol{A}(\boldsymbol{q}) \in \mathbb{R}^{\kappa \times n}$ and $\boldsymbol{b}(\boldsymbol{q}) \in \mathbb{R}^{\kappa}$. If $\boldsymbol{b}(\boldsymbol{q}) = \boldsymbol{0}$ the constraints are called catastatic, otherwise they are called acatastatic.

written in Pfaffian form as

$$\underbrace{\left[\, a_{i1}(\boldsymbol{q}) \;\dots\; a_{in}(\boldsymbol{q}) \,\right]}_{\boldsymbol{a}_i^\top(\boldsymbol{q})} \begin{bmatrix} \dot{q}_1 \\ \vdots \\ \dot{q}_n \end{bmatrix} = 0 \Rightarrow \boldsymbol{a}_i^\top(\boldsymbol{q})\dot{\boldsymbol{q}} = 0,$$

where $\boldsymbol{a}_i^\top(\boldsymbol{q}) = [a_{i1}(\boldsymbol{q}) \;\; a_{i2}(\boldsymbol{q}) \;\; \dots \;\; a_{in}(\boldsymbol{q})]$ is the i-th constraint vector, while $\kappa > 1$ constraints are written as

$$\boldsymbol{A}(\boldsymbol{q})\dot{\boldsymbol{q}} = \boldsymbol{0}, \tag{2}$$

where $\boldsymbol{A}(\boldsymbol{q}) \in \mathbb{R}^{\kappa \times n}$ is the constraint matrix.
The system (1) is additionally subject to λ nonlinear inequalities w.r.t. the state variables. Consider the continuous map $\boldsymbol{c} = (c_1, c_2, \dots, c_\lambda) : Q \to \mathbb{R}^\lambda$; then, the subset K of Q defined by the inequality constraints

$$K := \{\boldsymbol{q} \in Q \mid c_j(\boldsymbol{q}) \leq 0, \;\; j = 1, 2, \dots, \lambda\}, \tag{3}$$

is the viability set of the system, where $\mathcal{J}(\boldsymbol{q}) = \{j = 1, 2, \dots, \lambda \mid c_j(\boldsymbol{q}) = 0\}$ is the subset of active constraints.

2 Nonholonomic Control Design

The control design is based on our methodology [28] on the state feedback control for drift-free, kinematic nonholonomic systems of the form

$$\dot{\boldsymbol{q}} = \sum_{i=1}^{m} \boldsymbol{g}_i(\boldsymbol{q})u_i, \tag{4}$$

which are subject to kinematic Pfaffian constraints (2), where the state vector $\boldsymbol{q} \in \mathbb{R}^n$ includes the system generalized coordinates, $\boldsymbol{g}_i(\boldsymbol{q})$ are the control vector fields and u_i are the control inputs. The main idea is that one can define a smooth N-dimensional reference vector field $\mathbf{F}(\cdot)$ for (4), given by

$$\mathbf{F}(\boldsymbol{x}) = \lambda_{\mathrm{f}} \left(\boldsymbol{p}^\top \boldsymbol{x}\right) \boldsymbol{x} - \boldsymbol{p} \left(\boldsymbol{x}^\top \boldsymbol{x}\right), \tag{5}$$

where $\mathrm{N} \leq n$, $\lambda_{\mathrm{f}} \geq 2$, $\boldsymbol{x} \in \mathbb{R}^{\mathrm{N}}$ is a (particular) subvector of the configuration (state) vector $\boldsymbol{q} \in \mathbb{R}^n$, and $\boldsymbol{p} \in \mathbb{R}^{\mathrm{N}}$ is a vector that generates the vector field $\mathbf{F}(\cdot)$.
The dimension N of the vector field $\mathbf{F}(\cdot)$ is specified by the explicit form of the constraint equations, in the following sense: depending on the structure of $\boldsymbol{A}(\boldsymbol{q})$, the state space $\mathcal{Q}$ is trivially decomposed into $\mathcal{L} \times \mathcal{T}$, where $\mathcal{L}$ is the "leaf" space, $\mathcal{T}$ is the "fiber" space, $\dim\mathcal{L} = \mathrm{N}$, $n = \dim\mathcal{L} + \dim\mathcal{T}$. The local coordinates $\boldsymbol{x} \in \mathbb{R}^{\mathrm{N}}$ on the leaf are called leafwise states and the local coordinates $\boldsymbol{t} \in \mathbb{R}^{n-\mathrm{N}}$ on the fiber are called transverse states.
The vector field $\mathbf{F}(\cdot)$ is defined tangent to $\mathcal{L}$ in terms of the leafwise states $\boldsymbol{x}$, and is non-vanishing everywhere on $\mathcal{L}$ except for the origin $\boldsymbol{x} = \boldsymbol{0}$ of the local coordinate system, which by construction is the unique critical point of rose type [41]; this implies that all integral curves of $\mathbf{F}(\boldsymbol{x})$ contain the origin $\boldsymbol{x} = \boldsymbol{0}$. Thus, for $\mathrm{N} < n$, $\mathbf{F}(\cdot)$ is singular on the subset $\mathcal{A} = \{\boldsymbol{q} \in \mathbb{R}^n \mid \boldsymbol{x} = \boldsymbol{0}\}$; this singularity may necessitate switching for initial conditions $\boldsymbol{q_0} \in \mathcal{A}$. Input discontinuities are assumed to yield a closed loop vector field in (4) which is piecewise continuous. Solutions are then understood in the Filippov sense, i.e. $\dot{\boldsymbol{q}} \in \mathfrak{F}(\boldsymbol{q})$, where $\mathfrak{F}$ is a set valued map:

$$\mathfrak{F}(\boldsymbol{q}) \triangleq \overline{\mathrm{co}} \left\{ \lim \sum_{i=1}^{m} \boldsymbol{g}_i(\boldsymbol{q}_j)u_i : \boldsymbol{q}_j \to \boldsymbol{q}, \boldsymbol{q}_j \notin S_q \right\}$$

where $\overline{\mathrm{co}}$ stands for the convex closure and S_q is any set of measure zero [42].
Away from the singularity subset $\mathcal{A}$, $\mathbf{F}(\cdot)$ serves as a velocity reference for (4), i.e. at each $\boldsymbol{q} \in \mathcal{Q}$, the system vector field $\dot{\boldsymbol{q}} \in T_{\boldsymbol{q}}\mathcal{Q}$ is steered into the tangent space $T_{\boldsymbol{q}}\mathcal{L}$ of the integral curve of $\mathbf{F}(\cdot)$. In this sense, one can use the available control authority to steer the system vector field into the tangent bundle of the integral curves of $\mathbf{F}$, and "flow" in the direction of the reference vector field on its way to the origin. In [28] we show that these two objectives suggest the choice of particular Lyapunov-like functions V, and enable one to establish convergence of the system trajectories $\boldsymbol{q}(t)$ to the origin based on standard design and analysis techniques. In particular, one can find a smooth function $V(\boldsymbol{q}) : \mathbb{R}^n \to \mathbb{R}$ of compact level sets, and a state feedback control law $\boldsymbol{\gamma}(\cdot) = (\gamma_1(\cdot), \dots, \gamma_m(\cdot)) : \mathbb{R}^n \to \mathbb{R}^m$ such that

$$\dot{V} \leq 0 \;\; \Leftrightarrow \;\; \nabla V \, \dot{\boldsymbol{q}} = \nabla V \, \sum_{i=1}^{m} \boldsymbol{g}_i(\boldsymbol{q})\gamma_i(\cdot) \leq 0, \tag{6}$$

where $\nabla V \triangleq \begin{bmatrix} \frac{\partial V}{\partial q_1} & \dots & \frac{\partial V}{\partial q_n} \end{bmatrix}$ the gradient of V at $\boldsymbol{q}$. Convergence of the system trajectories $\boldsymbol{q}(t)$ to the origin is then established using standard tools.

3 Tools from Viability Theory

This section gives a brief description of concepts from viability theory [27,43] that are used in the paper.
Consider the dynamics of a system described by a (single-valued) map f from some open subset Ω of X to X, $f : \Omega \mapsto X$, where X is a finite dimensional vector space, and the initial value problem associated with the differential equation:

$$\forall t \in [0, T], \;\; \dot{x}\,(t) = f\big(x(t)\big), \;\;\; x(0) = x_0. \tag{7}$$

Definition 1 (*Viable Functions*) Let K be a subset of X. A function $x(\cdot)$ from $[0, T]$ to X is viable in K on $[0, T]$, if $x(t) \in K \; \forall t \in [0, T]$.
Definition 2 (*Viability Property*) Let K be a subset of Ω. K is said to be locally viable under f if, for any initial state $x_0 \in K$, there exist $T > 0$ and a viable solution on $[0, T]$ to the differential equation (7) starting at x_0. It is said to be (globally) viable under f if $T = \infty$.
The characterization of viable sets K under f is based on the concept of tangency: A subset K is viable under f if at each state x of K the velocity $f(x)$ is "tangent" to K at x, for bringing back a solution to the differential

equation inside K. An adequate concept of tangency is realized via the concept of the contingent cone.

Definition 3 (*Contingent Cone*) Let X be a normed space, K be a nonempty subset of X and x belong to K. The contingent cone to K at x is the set

$$T_K(x) = \left\{ v \in X \mid \liminf_{h \to 0+} \frac{d_K(x + hv)}{h} = 0 \right\},$$

where $d_K(y)$ denotes the distance of y to K, $d_K(y) := \inf_{z \in K} \|y - z\|$. Note that $\forall\ x \in \mathrm{Int}(K),\ T_K(x) = X$. Thus, if K is an open set, the contingent cone $T_K(x)$ to K at any $x \in K$, is always equal to the whole space.

(*Contingent Cone at a Fréchet differentiable point*) Consider the continuous real-valued map $g = (g_1, g_2, \ldots, g_p) : X \to \mathbb{R}^p$ and the subset K of X defined as

$$K = \{x \in X \mid g_i(x) \geq 0, \ \ i = 1, 2, \ldots, p\}, \tag{8}$$

where $g_i(\cdot)$ are Fréchet differentiable at x. For $x \in K$,

$$I(x) = \{i = 1, 2, \ldots, p \mid g_i(x) = 0\} \tag{9}$$

is the subset of active constraints. The contingent cone $T_K(x)$ to K is $T_K(x) = X$ whenever $I(x) = \emptyset$, otherwise

$$T_K(x) = \{v \in X \mid \forall i \in I(x),\ \langle g_i'(x), v\rangle \geq 0\},$$

where $g_i'(x) \in X^\star$ is the gradient of g_i at x, and $\langle \cdot, \cdot \rangle$ stands for the duality pairing.

Definition 4 (*Viability Domain*) Let K be a subset of Ω, then K is a viability domain of the map $f : \Omega \mapsto X$ if $\forall\ x \in K,\ f(x) \in T_K(x)$.

Definition 5 Consider a control system (U, f), defined by a feedback set-valued map $U : X \rightsquigarrow Z$, where X the state space and Z the control space, and a map $f : \mathrm{Graph}(U) \to X$, describing the dynamics of the system:

$$\dot{x}(t) = f(x(t), u(t)), \text{ where } u(t) \in U(x(t)).$$

We associate with any subset $K \subset \mathrm{Dom}(U)$ the regulation map $R_K := K \rightsquigarrow Z$ defined by

$$\forall x \in K, \ \ R_K(x) := \{u \in U(x) \mid f(x, u) \in T_K(x)\}.$$

Controls u belonging to $R_K(x)$ are called viable, and K is a viability domain if and only if the regulation map $R_K(x)$ has nonempty values.

If the subset K is given by (8), *the set of active constraints is as in* (9), *and for every $x \in K$, $\exists v_0 \in X$ such that $\forall i \in I(x),\ \langle g_i'(x), v_0\rangle \geq 0$, then the regulation map $R_K(x)$ is*

$$R_K(x) := \{u \in U(x) \mid \forall i \in I(x),\ \langle g_i'(x), f(x, u)\rangle \geq 0\}.$$

4 Viable Nonholonomic Controls

Consider a nonholonomic system of the form (4) subject to λ inequality state constraints determining a viability set K of the form (3), where $c_j(\cdot) : Q \to \mathbb{R}$ are continuously differentiable maps, $j \in \mathcal{J} = \{1, \ldots, \lambda\}$.

Assume that at some $\boldsymbol{q} \in K$ one has that $\mathcal{J}(\boldsymbol{q}) = \emptyset$, i.e. none of the constraints is active; then obviously $\boldsymbol{q} \in \mathrm{Int}(K)$, and the contingent cone of K at $\boldsymbol{q}$ coincides with the state space Q, $T_K(\boldsymbol{q}) = Q$.[3] This implies that the system can evolve along any direction $\dot{\boldsymbol{q}} \in T_{\boldsymbol{q}}Q$ without violating the viability constraints. For a nonholonomic system (4) with Pfaffian constraints (2), the admissible velocities $\dot{\boldsymbol{q}} \in T_{\boldsymbol{q}}Q$ belong into the null space of the constraint matrix $\boldsymbol{A}(\boldsymbol{q})$, which is an $(n - \kappa)$ dimensional subspace of the tangent space $T_{\boldsymbol{q}}Q$. Thus, at each $\boldsymbol{q} \in \mathrm{Int}(K)$, the viable admissible velocities $\dot{\boldsymbol{q}}$ for a nonholonomic system are tangent to an $(n - \kappa)$ dimensional subspace of the contingent cone $T_K(\boldsymbol{q})$.

Assume now that the j-th constraint becomes active at some point $\boldsymbol{z} \in \partial K$: $c_j(\boldsymbol{z}) = 0$, $j \in \mathcal{J}$, where ∂K stands for the boundary of the set K. The viable system velocities belong into the contingent cone of K at $\boldsymbol{z}$, $\dot{\boldsymbol{z}} \in T_K(\boldsymbol{z})$, which now is a subset (not necessarily a vector space but rather a cone) of the tangent space $T_{\boldsymbol{z}}Q$. Thus, an admissible velocity for a nonholonomic system (4) is viable at $\boldsymbol{z}$ if and only if

$$\dot{\boldsymbol{z}} \in \Big(\mathrm{Null}(\boldsymbol{A}(\boldsymbol{z})) \bigcap T_K(\boldsymbol{z})\Big) \neq \emptyset.$$

Based on these, we are able to characterize the conditions for selecting viable controls (if any) for the system (4). For $\boldsymbol{q} \in \mathrm{Int}(K)$, an admissible control $\boldsymbol{u} = (u_1, \ldots, u_m) : \mathbb{R}^n \to \mathbb{R}^m$ for (4) is viable at $\boldsymbol{q}$ if and only if

$$\boldsymbol{u} \in \boldsymbol{U}(\boldsymbol{q}), \quad \dot{\boldsymbol{q}} = \sum_{i=1}^{m} \boldsymbol{g}_i(\boldsymbol{q}) u_i \in T_K(\boldsymbol{q}) \triangleq T_{\boldsymbol{q}}Q,$$

which essentially implies that a control law $\boldsymbol{u}(\cdot)$ is viable at $\boldsymbol{q}$ as long as the control inputs u_i belong into the subset $\boldsymbol{U}(\boldsymbol{q})$ of feasible controls.

Assume now that $\boldsymbol{z} \in \partial K$ so that a single constraint is active: $c_j(\boldsymbol{z}) = 0$ for some $j \in \mathcal{J}$. The map of viable controls for a system (1) at $\boldsymbol{z}$ is:

$$R_K(\boldsymbol{z}) = \{\boldsymbol{u} \in \boldsymbol{U}(\boldsymbol{z}) \mid \langle c_j'(\boldsymbol{z}), \boldsymbol{f}(\boldsymbol{z}, \boldsymbol{u})\rangle \leq 0\},$$

where c_j' is the gradient of $c_j(\cdot)$ at $\boldsymbol{z}$, and $\langle \cdot, \cdot \rangle$ is the duality pairing. Following [44], the value of the duality pairing at $\boldsymbol{z}$ can be essentially expressed by the dot product $\nabla c_j\ \boldsymbol{f}(\boldsymbol{z}, \boldsymbol{u})$, where $\nabla c_j = \begin{bmatrix} \frac{\partial c_j}{\partial q_1} & \ldots & \frac{\partial c_j}{\partial q_n} \end{bmatrix}$ at $\boldsymbol{z} \in \partial K$. The regulation map then reads:

$$R_K(\boldsymbol{z}) = \{\boldsymbol{u} \in \boldsymbol{U}(\boldsymbol{z}) \mid \nabla c_j \boldsymbol{f}(\boldsymbol{z}, \boldsymbol{u}) \leq 0\}.$$

Thus, an admissible control $\boldsymbol{u} = (u_1, \ldots, u_m) : \mathbb{R}^n \to$

[3] If K is a differentiable manifold, then the contingent cone $T_K(\boldsymbol{q})$ coincides with the tangent space to K at $\boldsymbol{q}$.

$\mathbb{R}^m$ for (4) is viable at $\boldsymbol{z} \in \partial K$ if and only if

$$\boldsymbol{u}(\boldsymbol{z}) \in \boldsymbol{U}(\boldsymbol{z}),\ \left[\frac{\partial c_j}{\partial q_1}\ \dots\ \frac{\partial c_j}{\partial q_n}\right] \sum_{i=1}^{m} \boldsymbol{g}_i(\boldsymbol{z}) u_i \leq 0. \quad (10)$$

It immediately follows that if more than one constraints $c_j(\cdot) : Q \to \mathbb{R}$ are simultaneously active at some $\boldsymbol{z} \in \partial K$, then a control law $\boldsymbol{u}(\cdot)$ is viable at $\boldsymbol{z}$ if the condition (10) is satisfied for each one of the active constraints. If *all* λ constraints are active at $\boldsymbol{z}$, the viability conditions are written in matrix form as

$$\boldsymbol{u}(\boldsymbol{z}) \in \boldsymbol{U}(\boldsymbol{z}), \quad \mathbf{J}_{\boldsymbol{c}}(\boldsymbol{z}) \sum_{i=1}^{m} \boldsymbol{g}_i(\boldsymbol{z}) u_i \leq \mathbf{0}, \quad (11)$$

where $\mathbf{J}_{\boldsymbol{c}}(\boldsymbol{z})$ is the Jacobian matrix of the map $\boldsymbol{c} = (c_1(\cdot), \dots, c_\lambda(\cdot)) : Q \to \mathbb{R}^\lambda$, evaluated at $\boldsymbol{z} \in \partial K$.
Consequently, a control law $\boldsymbol{\gamma}(\cdot) = (\gamma_1(\cdot), \dots, \gamma_m(\cdot)) : \mathbb{R}^n \to \mathbb{R}^m$ is viable at $\boldsymbol{z} \in \partial K$ if and only if

$$\boldsymbol{\gamma}(\boldsymbol{z}) \in \boldsymbol{U}(\boldsymbol{z}),\ \left[\frac{\partial c_j}{\partial q_1}\ \dots\ \frac{\partial c_j}{\partial q_n}\right] \sum_{i=1}^{m} \boldsymbol{g}_i(\boldsymbol{z}) \gamma_i(\boldsymbol{z}) \leq 0, \quad (12)$$

for each one of the active constraints $c_j(\boldsymbol{z}) = 0$, where $\boldsymbol{U}(\boldsymbol{z}) \subseteq \mathbb{R}^m$ is the subset of feasible controls at $\boldsymbol{z}$.
To illustrate the viability condition (10) let us consider the case when a single constraint is active: $c_j(\boldsymbol{z}) = 0$, $\boldsymbol{z} \in \partial K$ (Fig. 1). The viable system velocities $\dot{\boldsymbol{z}}$ belong into the contingent cone $T_K(\boldsymbol{z})$ at $\boldsymbol{z}$; thus, any control $\boldsymbol{u} = (u_1, \dots, u_m) \in \boldsymbol{U}(\boldsymbol{z})$ such that $\dot{\boldsymbol{z}} = \sum_{i=1}^{m} \boldsymbol{g}_i(\boldsymbol{z}) u_i \in T_K(\boldsymbol{z})$ is viable. Furthermore, following [28], the system velocities that establish asymptotic convergence to the origin define the subset $\mathcal{C} = \{\dot{\boldsymbol{z}} \in T_{\boldsymbol{z}} Q \mid \nabla V \dot{\boldsymbol{z}} \leq 0\}$. Thus, a convergent control law $\boldsymbol{\gamma}(\cdot)$ is also viable at $\boldsymbol{z} \in \partial K$ if and only if $\boldsymbol{\gamma}(\boldsymbol{z}) \in \boldsymbol{U}(\boldsymbol{z})$ and furthermore the system velocity $\dot{\boldsymbol{z}} = \sum_{i=1}^{m} \boldsymbol{g}_i(\boldsymbol{z}) \gamma_i(\boldsymbol{z})$ belongs into the intersection $(\mathcal{C} \bigcap T_K(\boldsymbol{z}))$; if this intersection is empty, then any convergent solution $\boldsymbol{\gamma}(\cdot)$ steers the system trajectories out of K.
Therefore, given the state feedback control solutions in [28], the idea for designing viable feedback control laws for the class of nonholonomic systems (1) reduces into redesigning (if necessary) the convergent control laws $\boldsymbol{\gamma}(\cdot) : \mathbb{R}^n \to \mathbb{R}^m$ by means of switching control, so that they yield viable control inputs $\boldsymbol{u}(\boldsymbol{z})$, $\forall \boldsymbol{z} \in \partial K$. The proposed control design is illustrated via the following example.

5 Viable control design for an underactuated marine vehicle with limited sensing

We consider the motion control on the horizontal plane for an underactuated marine vehicle subject to configuration constraints, which mainly arise because of the onboard vision-based sensor system. The sensor suite consists of a camera and two laser pointers mounted on the vehicle, and provides the vehicle's position and orientation (pose) vector $\boldsymbol{\eta} = [x\ \ y\ \ \psi]^\top$ w.r.t. a global coordi-

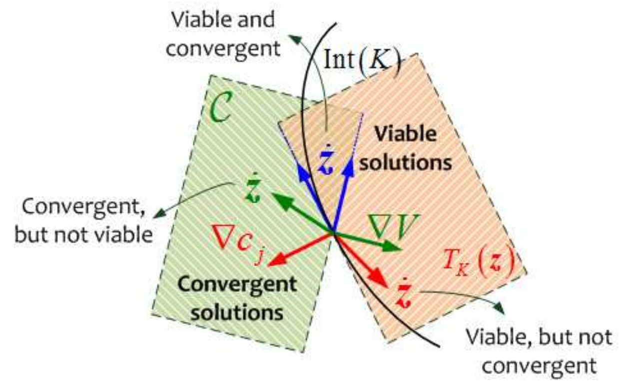

Fig. 1. Any control law $\boldsymbol{\gamma}(\cdot) = (\gamma_1(\cdot), \dots, \gamma_m(\cdot)) : \mathbb{R}^n \to \mathbb{R}^m$ such that $\boldsymbol{\gamma}(\boldsymbol{z}) \in \boldsymbol{U}(\boldsymbol{z})$, $\dot{\boldsymbol{z}} = \sum_{i=1}^{m} \boldsymbol{g}_i(\boldsymbol{z}) \gamma_i(\cdot) \in (\mathcal{C} \bigcap T_K(\boldsymbol{z}))$ is also viable at $\boldsymbol{z} \in \partial K$, bringing the system trajectories into the interior of K.

nate frame $\mathcal{G}$, which lies on the center of a target on a vertical surface (Fig. 2). The target and the two laser dots

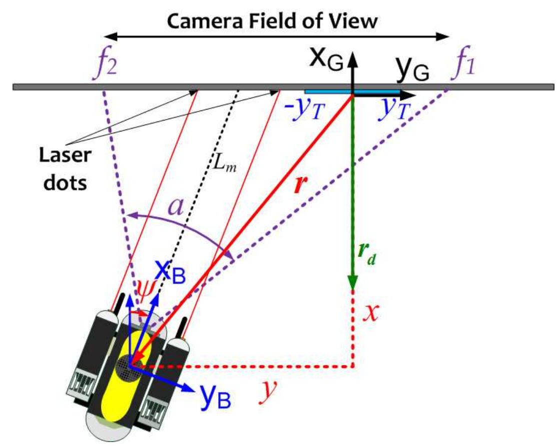

Fig. 2. Modeling of the state constraints

projected on the surface are tracked using computer vision algorithms and this information is used to estimate the pose vector $\boldsymbol{\eta}$. Thus, the target and the laser dots should always be visible in the camera f.o.v., for the sensor system to be effective. These requirements impose a set of nonlinear inequality constraints w.r.t. $\boldsymbol{\eta}$, which are treated as viability constraints that define a viability set K for the system. The control objective is thus defined as to control the vehicle so that it converges into a set $G \subset K$ of desired configurations $\boldsymbol{\eta_d} \in G$, while the system trajectories $\boldsymbol{\eta}(t)$ never escape K.

5.1 Mathematical Modeling

The marine vehicle has two back thrusters for moving along the surge and the yaw degree of freedom (d.o.f.), but no side (lateral) thruster for moving along the sway d.o.f.. Following [45] the kinematic and dynamic equations of motion are analytically written as:

$$\dot{x} = u \cos\psi - v \sin\psi \quad (13a)$$
$$\dot{y} = u \sin\psi + v \cos\psi \quad (13b)$$

$$\dot{\psi} = r \quad (13c)$$
$$m_{11}\dot{u} = m_{22}vr + X_u u + X_{u|u|}\,|u|\,u + \tau_u \quad (13d)$$
$$m_{22}\dot{v} = -m_{11}ur + Y_v v + Y_{v|v|}\,|v|\,v \quad (13e)$$
$$m_{33}\dot{r} = (m_{11} - m_{22})uv + N_r r + N_{r|r|}\,|r|\,r + \tau_r, \quad (13f)$$

where $\boldsymbol{\eta} = \left[\boldsymbol{r}^\top\ \psi\right]^\top = [x\ \ y\ \ \psi]^\top$ is the pose vector of the vehicle w.r.t. the global frame $\mathcal{G}$, $\boldsymbol{r} = [x\ \ y]^\top$ is the position vector and ψ is the orientation of the vehicle w.r.t. $\mathcal{G}$, $\boldsymbol{\nu} = [u\ \ v\ \ r]^\top$ is the vector of linear and angular velocities in the body-fixed coordinate frame $\mathcal{B}$, m_{11}, m_{22}, m_{33} are the terms of the inertia matrix (including the added mass effect) along the axes of frame $\mathcal{B}$, X_u, Y_v, N_r are the linear drag terms, $X_{u|u|}$, $Y_{v|v|}$, $N_{r|r|}$ are the nonlinear drag terms, and τ_u, τ_r are the control inputs along the surge and yaw d.o.f.. [4]

5.2 Nonholonomic control design

The system (13) falls into the class of control affine underactuated mechanical systems with drift: $\dot{\mathbf{x}} = \mathbf{f}(\mathbf{x}) + \sum_{i=1}^{m} \mathbf{g}_i(\mathbf{x})\mathrm{u}_i$, where $\mathbf{x} = [x\ \ y\ \ \psi\ \ u\ \ v\ \ r]^\top$ is the state vector, including the generalized coordinates $\boldsymbol{\eta}$ and the body-fixed velocities $\boldsymbol{\nu}$, and $\mathrm{u}_1 = \tau_u$, $\mathrm{u}_2 = \tau_r$ are the control inputs, respectively. The dynamics of the sway d.o.f. (13e) serve as a second-order (dynamic) nonholonomic constraint. If we only consider the kinematic subsystem for a moment, we see that (13a), (13b) are combined into $-\dot{x}\sin\psi + \dot{y}\cos\psi = v \Rightarrow$

$$\underbrace{[-\sin\psi\ \ \cos\psi\ \ 0]}_{\boldsymbol{a}^\top(\boldsymbol{\eta})}\begin{bmatrix}\dot{x}\\ \dot{y}\\ \dot{\psi}\end{bmatrix} = v \Rightarrow \boldsymbol{a}^\top(\boldsymbol{\eta})\dot{\boldsymbol{\eta}} = v, \quad (14)$$

which for $v \neq 0$ can be seen as an acatastatic Pfaffian constraint on the unicycle. The constraint equation (14) implies that $\boldsymbol{\eta} = \mathbf{0}$ is an equilibrium point if and only if $v\,|_{\boldsymbol{\eta}=\mathbf{0}} = 0$, i.e. if and only if (14) turns into catastatic at the origin $\boldsymbol{\eta} = \mathbf{0}$.

With this insight, one can try to steer the kinematic subsystem augmented with the second order constraint (13e) to the origin $\boldsymbol{\eta} = \mathbf{0}$, using the velocities u, r as virtual control inputs, while ensuring that the velocity v vanishes at $\boldsymbol{\eta} = \mathbf{0}$. Thus, the system (13) can be divided into two subsystems Σ_1, Σ_2, where Σ_1 consists of the kinematic equations (13a)-(13c) and the sway dynamics (13e), while the dynamic equations (13d), (13f) constitute the subsystem Σ_2. The velocities u, r are considered as virtual control inputs for Σ_1, while the actual control inputs τ_u, τ_r are used to control Σ_2.

The constraint (14) can now be used to apply the steps presented in [28], in order to design the virtual control inputs for Σ_1: based on the structure of the constraint vector $\boldsymbol{a}^\top(\boldsymbol{\eta})$, the states $\boldsymbol{r} = [x\ \ y]^\top \triangleq \boldsymbol{x}$ are the *leafwise* states while ψ is the *transverse* state. Thus, an $\mathrm{N} = 2$ dimensional reference vector field $\mathbf{F}(\cdot) = \mathrm{F}_x \frac{\partial}{\partial x} + \mathrm{F}_y \frac{\partial}{\partial y}$ can be picked out of (5), in terms of the leafwise states x, y. For $\lambda_\mathrm{f} = 3$ and $\boldsymbol{p} = [1\ \ 0]^\top$, the vector field reads:

$$\mathrm{F}_x = 2x^2 - y^2, \quad \mathrm{F}_y = 3xy. \quad (15)$$

The vector field (15) is non-vanishing everywhere in $\mathbb{R}^2$ except for the origin $\boldsymbol{r} = \mathbf{0}$, and has integral curves that all converge to $\boldsymbol{r} = \mathbf{0}$ with direction $\phi \to 0$. Thus, the vehicle can be controlled so that it aligns with the direction and flows along the integral curves of the vector field $\mathbf{F}(\cdot)$, until it converges to $\boldsymbol{\eta} = \mathbf{0}$. Note that for the integral curves to converge to the desired configuration $\boldsymbol{\eta_d} = [x_d\ \ y_d\ \ 0]^\top$, the reference vector field $\mathbf{F}(\cdot)$ is defined out of (5) in terms of the position error $\boldsymbol{r_1} = \boldsymbol{r} - \boldsymbol{r_d}$; thus, the vector field components read:

$$\mathrm{F}_x = 2{x_1}^2 - {y_1}^2, \quad \mathrm{F}_y = 3x_1y_1, \quad (16)$$

where $\boldsymbol{r_1} = [x_1\ \ y_1]^\top$, $x_1 = x - x_d$, $y_1 = y - y_d$.

Theorem 1 The trajectories $\boldsymbol{\eta}(t) = [x(t)\ \ y(t)\ \ \psi(t)]^\top$ of the subsystem Σ_1 globally converge to the desired configuration $\boldsymbol{\eta_d} = [x_d\ \ y_d\ \ 0]^\top$ under the control laws $u = \gamma_1(\cdot)$, $r = \gamma_2(\cdot)$:

$$\gamma_1(\cdot) = -k_1\,\mathrm{sgn}\left(\boldsymbol{r_1}^\top \begin{bmatrix}\cos\psi\\ \sin\psi\end{bmatrix}\right)\tanh\left(\mu\|\boldsymbol{r_1}\|\right), \quad (17a)$$
$$\gamma_2(\cdot) = -k_2(\psi - \phi) + \dot{\phi}, \quad (17b)$$

where $k_1, k_2 > 0$, $\phi = \mathrm{atan2}(\mathrm{F}_y, \mathrm{F}_x)$ is the orientation of the vector field (16) at (x, y) and the function $\mathrm{sgn}(\cdot) : \mathbb{R} \to \{-1, 1\}$ is defined as: $\mathrm{sgn}(a) = \begin{cases} 1, & \text{if } a \geq 0,\\ -1, & \text{if } a < 0.\end{cases}$

The proof is given in the Appendix A.

Finally, the control inputs τ_u, τ_r of the subsystem Σ_2 should be designed so that the actual velocities $u(t)$, $r(t)$ are globally exponentially stable (GES) to the virtual control inputs $\gamma_1(\cdot)$, $\gamma_2(\cdot)$.

Theorem 2 The actual velocities $u(t)$, $r(t)$ are GES to the virtual control inputs $\gamma_1(\cdot)$, $\gamma_2(\cdot)$, respectively, under the control laws $\tau_u = \xi_1(\cdot)$, $\tau_r = \xi_2(\cdot)$ given as:

$$\tau_u = m_{11}\alpha - m_{22}vr - X_u u - X_{u|u|}|u|u, \quad (18a)$$
$$\tau_r = m_{33}\beta - (m_{11} - m_{22})ur - N_r r - N_{r|r|}|r|r, \quad (18b)$$

where

$$\alpha = -k_u(u - \gamma_1(\cdot)) + (\nabla\gamma_1)\dot{\boldsymbol{\eta}}, \quad k_u > 0, \quad (19a)$$
$$\beta = -k_r(r - \gamma_2(\cdot)) + (\nabla\gamma_2)\dot{\boldsymbol{\eta}}, \quad k_r > 0, \quad (19b)$$

and $\nabla\gamma_\mathtt{k} = \left[\frac{\partial\gamma_\mathtt{k}}{\partial x}\ \ \frac{\partial\gamma_\mathtt{k}}{\partial y}\ \ \frac{\partial\gamma_\mathtt{k}}{\partial\psi}\right]$ is the gradient of $\gamma_\mathtt{k}$, $\mathtt{k} = 1, 2$. The proof is given in the Appendix B.

[4] The model (13) is valid under the assumption that the inertia and damping matrices are diagonal, i.e. for bodies with three planes of symmetry, performing non-coupled motions at low speed [45]. In general, these assumptions are considered as a good approximation for dynamic positioning, however they still introduce uncertainty in the model.

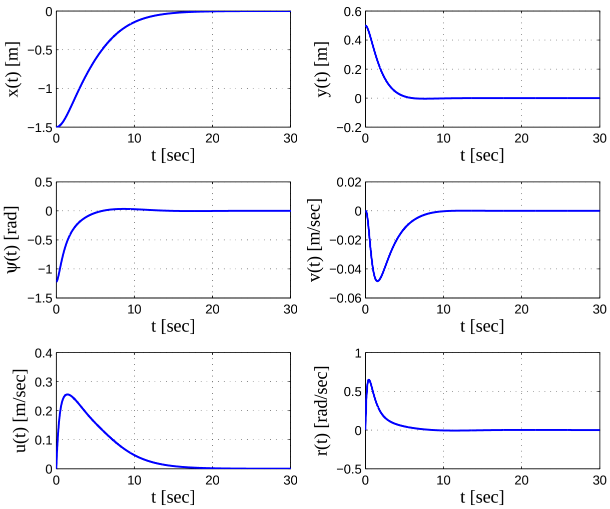

Fig. 3. Response of the system trajectories $\mathbf{x}(t)$.

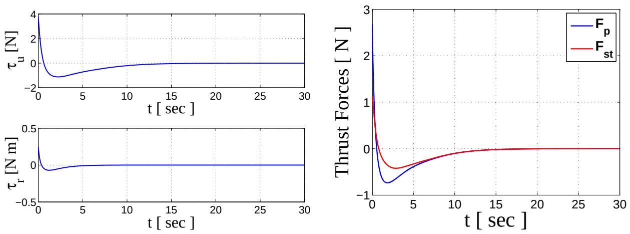

(a) The control inputs (18) (b) Thrust Forces

Fig. 4. The resulting control inputs and thrust forces.

The system trajectories $\mathbf{x}(t)$ under the control law (18), (19), (17) are shown in Fig. 3, whereas the control inputs τ_u, τ_r and the resulting thrust forces F_p, F_{st} are shown in Fig. 4(a) and Fig. 4(b), respectively.

5.3 *Viable nonholonomic control design*

The viability set K of the system (13) is determined by the following requirements (Fig. 2):

- The target should always be in the camera f.o.v., $[-y_T, y_T] \subseteq [f_2, f_1]$, so that sensing is effective.
- The laser range L_m must be within given bounds, $L_{\min} \leq L_m \leq L_{\max}$, so that the laser dots on the surface can be effectively detected.

These specifications impose $\lambda = 4$ nonlinear inequality constraints of the form $c_j(x, y, \psi) \leq 0$, $j \in \mathcal{J} = \{1, 2, 3, 4\}$, written analytically as

$$c_1 : y - x\tan(\psi - \alpha) + y_T \leq 0, \tag{20a}$$
$$c_2 : y_T - y + x\tan(\psi + \alpha) \leq 0, \tag{20b}$$
$$c_3 : L_{\min} + \frac{x}{\cos\psi} \leq 0, \tag{20c}$$
$$c_4 : -\frac{x}{\cos\psi} - L_{\max} \leq 0. \tag{20d}$$

Note that the control law (17) yields solutions that, starting from any initial configuration $\boldsymbol{\eta_0}$ in K converge to (any) desired configuration $\boldsymbol{\eta_d}$ in K. Nevertheless, the convergent trajectories $\boldsymbol{\eta}(t)$ may not be viable in K, in the sense that the control inputs may steer the trajectories $\boldsymbol{\eta}(t)$ out of K during some finite time.

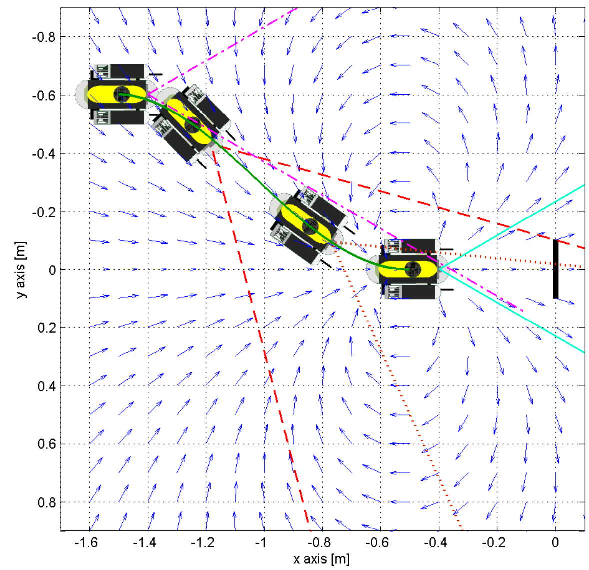

Fig. 5. A convergent solution $\boldsymbol{\eta}(t)$ given by the control law (17) may violate viability during some (finite) time interval.

Such an example is shown in Fig. 5. Assume for now that only the constraint $c_1(\cdot)$ (20a) is of interest. The vehicle starts on a configuration $\boldsymbol{\eta_0}$ in K; however, tracking the reference vector field $\mathbf{F}(\cdot)$ under (17) on its way to $\boldsymbol{\eta_d} = [-0.5 \;\; 0 \;\; 0]^\top$ implies that the convergent trajectories $\boldsymbol{\eta}(t)$ are driven out of K for some finite time. More specifically, the constraint $c_1(\cdot)$ becomes active when the target lies on the left boundary of the f.o.v. (Fig. 5, dashed line). This condition defines a subset $\mathcal{Z}_1 = \{\boldsymbol{z} \in \partial K \mid c_1(\cdot) = y - x\tan(\psi - \alpha) + y_T = 0\}$ of ∂K. From the definition of the regulation map $R_K(\cdot)$ (Section 3) one has that the viable system velocities at $\boldsymbol{z} \in \mathcal{Z}_1$ satisfy $\nabla c_1 \dot{\boldsymbol{z}} \leq 0 \Rightarrow \left[-\tan(\psi-\alpha) \;\; 1 \;\; -x\sec^2(\psi-\alpha) \right] \begin{bmatrix} \dot{x} \\ \dot{y} \\ \dot{\psi} \end{bmatrix} \leq 0.$ Substituting the system equations yields:

$$(-\tan(\psi - \alpha)\cos\psi + \sin\psi)u + (\tan(\psi - \alpha)\sin\psi + \cos\psi)\,v - x\sec^2(\psi - \alpha)r \leq 0. \tag{21}$$

The viability condition (21) verifies that the control inputs (17) violate the constraint $c_1(\boldsymbol{z}) = 0$: at $\boldsymbol{z} \in \mathcal{Z}_1$ the vehicle moves with $u, r, \psi > 0$, thus the first and third term are > 0, whereas the (in general indefinite) velocity v is not negative enough to satisfy (21). Therefore, the control laws $u = \gamma_1(\cdot)$, $r = \gamma_2(\cdot)$ should be redesigned so that (21) holds $\forall \boldsymbol{z} \in \mathcal{Z}_1$.

To this end, the condition (21) offers the way to select viable control inputs when $\boldsymbol{z} \in \mathcal{Z}_1$. If the system starts at $\boldsymbol{z}$ with zero linear and angular velocities, then a viable option is to set $u(\boldsymbol{z}) = 0$ and $r(\boldsymbol{z}) < 0$; then, one has $v = 0$ since (13e) reduces to $\dot{v} = 0$, and the condition (21) is satisfied, since always $x < 0$.[5] For picking a viable control input $r(\boldsymbol{z})$, one can choose to regulate the orientation ψ of the vehicle to the angle $\phi_t = \text{atan2}(-y, -x)$, which essentially is the orientation of the vector $-\boldsymbol{\eta}$ that connects the vehicle with the target via the angular velocity $r_{viab_1} = -k(\psi - \phi_t)$. In this way, the system is controlled so that target is centered in the camera f.o.v., avoiding thus the left boundary.

Similarly, the viability conditions when the remaining constraints become active at some $\mathcal{Z}_j = \{\boldsymbol{z} \mid c_j(\boldsymbol{z}) = 0\}$, $j \in \{2, 3, 4\}$, are analytically written as:

$$\nabla c_2 \dot{\boldsymbol{\eta}} \leq 0 \Rightarrow \left[\tan(\psi+\alpha) \quad -1 \quad x\sec^2(\psi+\alpha)\right] \dot{\boldsymbol{\eta}} \leq 0 \overset{(13)}{\Rightarrow} \\ (\tan(\psi+\alpha)\cos\psi - \sin\psi)\, u + x\sec^2(\psi+\alpha) r - \\ - (\tan(\psi+\alpha)\sin\psi + \cos\psi)\, v \leq 0, \tag{22a}$$

$$\nabla c_3 \dot{\boldsymbol{\eta}} \leq 0 \Rightarrow [\sec\psi \quad 0 \quad x]\, \dot{\boldsymbol{\eta}} \leq 0 \overset{(13)}{\Rightarrow} \\ u + x\, r - \tan\psi\, v \leq 0, \tag{22b}$$

$$\nabla c_4 \dot{\boldsymbol{\eta}} \leq 0 \Rightarrow [-\sec\psi \quad 0 \quad -x]\, \dot{\boldsymbol{\eta}} \leq 0 \overset{(13)}{\Rightarrow} \\ \tan\psi\, v - u - x\, r \leq 0, \tag{22c}$$

and indicate how to select viable control laws for the case that the corresponding constraint becomes active. Thus, if $\boldsymbol{z} \in \mathcal{Z}_2$, i.e. if the target is adjacent to the right boundary of the f.o.v., the system can be as well controlled so that the target is centered in the camera f.o.v. via $r_{viab_2} = -k(\psi - \phi_t)$; in this case the resulting angular velocity is $r_{viab_2} > 0$; given that $x < 0$ and by choosing the control gain k large enough, the term involving r is negative and dominates the remaining terms in (22a). In the same spirit, for the remaining constraints one can verify that by setting $r_{viab_{3,4}} = 0$ and $u_{viab_{3,4}}$ by (17a) the term involving u is negative, implying that viability is maintained.

Thus, for redesigning the control laws (17) so that they are viable at $\boldsymbol{z} \in \mathcal{Z}_j$, $j \in \mathcal{J}$, one can consider the continuous switching signal

$$\sigma_j(c_j) = \begin{cases} \frac{c_j}{c_{j^*}}, & \text{if } c_{j^*} \leq c_j \leq 0, \\ 1, & \text{if } c_j < c_{j^*}, \end{cases} \tag{23}$$

shown in Fig. 5, and use the control law:

$$u = \sigma_j(c_j) u_{conv} + (1 - \sigma_j(c_j)) u_{viab_j}, \tag{24a}$$

$$r = \sigma_j(c_j) r_{conv} + (1 - \sigma_j(c_j)) r_{viab_j}, \tag{24b}$$

where c_{j^*} is a critical value for the constraint $c_j(\cdot)$, u_{conv}, r_{conv} are the convergent to the origin control laws given by (17) and u_{viab_j}, r_{viab_j} are viable control laws at $\boldsymbol{z} \in \mathcal{Z}_j$. Then, if $c_j(\boldsymbol{z}) = 0$ one has $\sigma_j(c_j) = 0$, which ensures that the control laws given by (24) at $\boldsymbol{z} \in \mathcal{Z}_j$ are viable.

[5] This is not the only viable option; any control input $[u \;\; r]^\top \in \boldsymbol{U}(\boldsymbol{z})$ such that $\nabla c_1 \dot{\boldsymbol{z}} \leq 0$ implies that the constraint $c_1(\boldsymbol{z})$ is not violated.

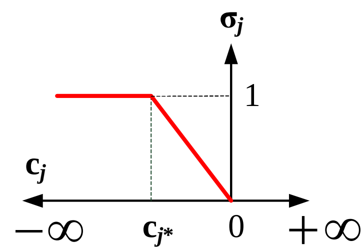

Fig. 6. The switching signal $\sigma_j(c_j)$.

Under this control setting, if the system trajectories $\boldsymbol{\eta}(t)$ evolve away from the subset $\mathcal{Z}_j \in \partial K$ so that $c_j(\boldsymbol{\eta}(t)) < c_{j^*}(\boldsymbol{\eta}(t))\ \forall j \in \mathcal{J}\ \forall t \geq 0$, then the viable controls are never activated and the system is guaranteed to converge to the desired configuration $\boldsymbol{\eta_d}$ under the convergent control law (17). On the other hand, if the switch $\sigma_j(\cdot)$ is activated at some $t \geq 0$, then the vehicle does not track the convergent to $(x, y) = (0, 0)$ integral curves of the vector field $\mathbf{F}$ during the time interval that $\sigma_j(c_j) \neq 1$. If furthermore the corresponding viable control laws are not convergent to $\boldsymbol{\eta_d}$, then the system is no longer guaranteed to converge to $\boldsymbol{\eta_d}$. In this case, one can relax the requirement on the convergence to a single point, and rather choose to establish convergence to a goal set $G \subset K$ of desired configurations, given as $G = \left\{\boldsymbol{\eta_d} \in K \;\middle|\; {x_d}^2 + {y_d}^2 = d^2, \psi_d = \text{atan2}(-y_d, -x_d)\right\}$, where d is a desired distance w.r.t. the target. The viable linear velocity controller is given as

$$u_{viab} = -k_1 \,\text{sgn}\left([x_1 \;\; y_1] \begin{bmatrix} \cos\psi \\ \sin\psi \end{bmatrix}\right) \tanh(\mu \|\boldsymbol{r_1}\|), \tag{25}$$

where $\boldsymbol{r_1} = [x_1 \;\; y_1]^\top$, $x_1 = x - x_d$, $y_1 = y - y_d$, $x_d = d\cos\psi_d$, $y_d = d\sin\psi_d$, $\psi_d = \text{atan2}(-y, -x)$.

The orchestration of the switching between convergent and viable control laws taking into consideration all j constraints can be implemented by replacing the switching signal $\sigma_j(c_j)$ with the switching signal $\sigma^* := \min(\sigma_j)$, $j \in \mathcal{J}$;

$$u = \min(\sigma_j) u_{conv} + (1 - \min(\sigma_j)) u_{viab_j}, \tag{26a}$$

$$r = \min(\sigma_j) r_{conv} + (1 - \min(\sigma_j)) r_{viab_j}, \tag{26b}$$

In this way, the system switches when necessary to the viable controls u_{viab_j}, r_{viab_j} that correspond to the constraint j which is closer to be violated.

Finally, note that the control gains k_1, k_2, k_u, k_r can be properly tuned so that the virtual control inputs u, r correspond to thrust forces F_p, F_{st} that belong into the compact set $\mathcal{U} = [-f_p, f_p] \times [-f_{st}, f_{st}]$.

To evaluate the efficacy of the methodology, let us consider the scenario shown in Fig. 7. The vehicle initiates on a configuration $\boldsymbol{\eta_0}$ where both the constraints $c_2(\cdot)$, $c_4(\cdot)$ are active. Thus, a viable control law that does not violate both (22a), (22c) is active at $t = 0$; in this case, we chose to use the convergent control law (17) as a viable control law, with the control gains k_1, k_2 tuned so that

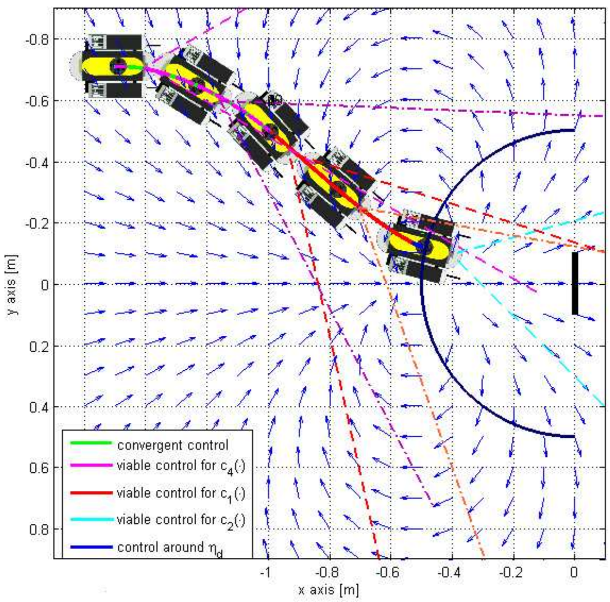

Fig. 7. The path $x(t)$, $y(t)$ under the control scheme (26). The vehicle converges into a point of the goal set G.

none of the constraints is violated. The vehicle moves towards the nominal desired configuration $\boldsymbol{\eta_d}$ under (26); note that the constraints $c_4(\cdot)$, $c_1(\cdot)$ become nearly active during some time intervals, activating the corresponding viable control laws. The vehicle approaches the goal set G under (26) for $j = 1$, i.e. by regulating the orientation ψ so that the target is always visible (red path). In this scenario the effect of the viable control law for $c_1(\cdot)$ does not vanish, and thus the vehicle does not converge to $\boldsymbol{\eta_d} = [-0.5 \;\; 0 \;\; 0]^\top$, but rather to a configuration in G. Finally, to ensure that the vehicle will stabilize at some point in G, the system switches to the viable control law corresponding to $j = 1$ in a small ball around $\boldsymbol{r_d}$ (blue path).

The evolution of the constraint functions $c_j(\boldsymbol{\eta}(t))$, $j \in \mathcal{J}$ is shown in Fig. 8; the value of $c_j(\cdot)$ is always non-positive which implies that viability is always maintained.

Finally, Fig. 9 shows the resulting path under (26) for a case that the vehicle starts on a point in K, so that the viable control laws are not active (green path). As the vehicle moves towards $\boldsymbol{\eta_d}$ the switching signal $\sigma^* = \sigma_2$ becomes < 1, activating the corresponding viable control law for some finite time interval (red path). The vehicle moves away from the corresponding boundary $\mathcal{Z}_2$ of the set K, yielding $\sigma^* = 1$, and thus eventually converges to $\boldsymbol{\eta_d}$ under the convergent control law.

6 Viable control under a class of bounded disturbances

6.1 Robust nonholonomic control design

Let us now assume that the vehicle moves in the presence of an irrotational current of velocity V_c and direction β_c w.r.t. $\mathcal{G}$. As it will be shown later, the current V_c, β_c does not have to be explicitly known or constant, but rather to correspond to a class of bounded perturbations so that

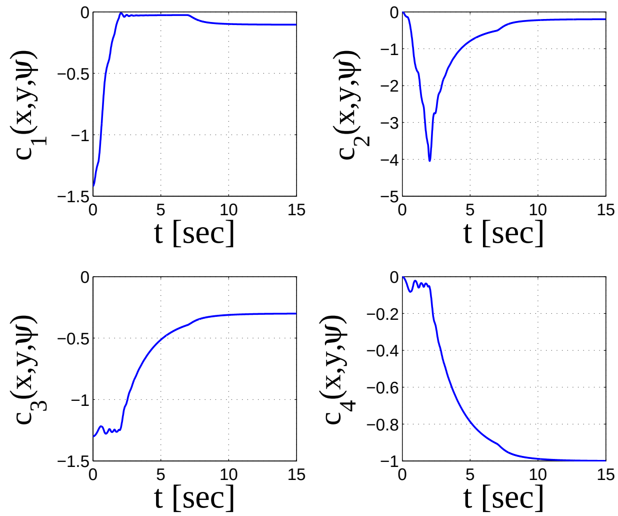

Fig. 8. The value of the constraints remains always negative.

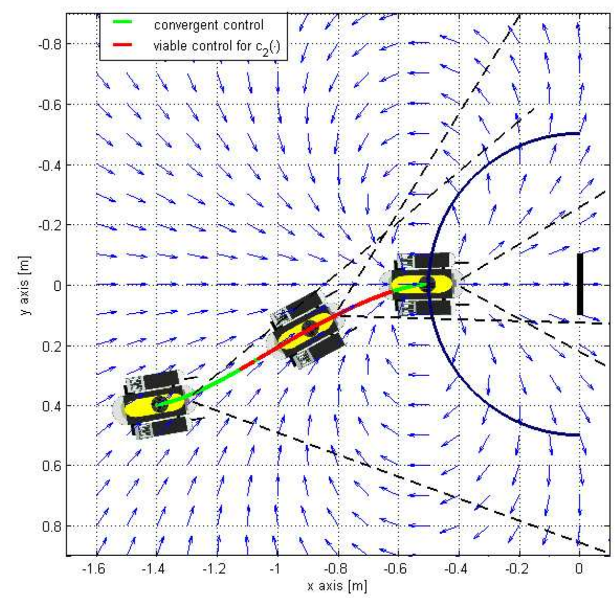

Fig. 9. The vehicle starts moving under the control law (24) where $\sigma^* = 1$, i.e. the convergent control law (17) is active (green path). When the constraint $c_2(\cdot)$ is nearly violated the corresponding switching signal σ_2 becomes < 1 for some time interval (red path). The vehicle eventually converges to $\boldsymbol{\eta_d} = [-0.5 \;\; 0 \;\; 0]^\top$.

the velocity is at most equal to a known upper bound. Following [45], the kinematic and dynamic equations of motion are rewritten including the current effect as:

$$\dot{x} = u_r \cos\psi - v_r \sin\psi + V_c \cos\beta_c \tag{27a}$$
$$\dot{y} = u_r \sin\psi + v_r \cos\psi + V_c \sin\beta_c \tag{27b}$$
$$\dot{\psi} = r \tag{27c}$$
$$m_{11}\dot{u}_r = m_{22} v_r r + X_u u_r + X_{u|u|} |u_r| \, u_r + \tau_u \tag{27d}$$
$$m_{22}\dot{v}_r = -m_{11} u_r r + Y_v v_r + Y_{v|v|} |v_r| \, v_r \tag{27e}$$
$$m_{33}\dot{r} = (m_{11} - m_{22}) \, u_r v_r + N_r r + N_{r|r|} |r| \, r + \tau_r \tag{27f}$$

where $\boldsymbol{\nu_r} = [u_r \;\; v_r \;\; r]^\top$ is the vector of the relative velocities in the body-fixed frame $\mathcal{B}$, $\boldsymbol{\nu_r} = \boldsymbol{\nu} - \boldsymbol{\nu_c}$ and $\boldsymbol{\nu_c} = [V_c \cos(\beta_c - \psi) \;\; V_c \sin(\beta_c - \psi) \;\; 0]^\top$ are the current velocities w.r.t. frame $\mathcal{B}$.
The system is written as a control affine system with drift vector field $\mathbf{f}(\mathbf{x})$ and additive perturbations $\boldsymbol{\delta}(\cdot)$ as: $\dot{\mathbf{x}} = \mathbf{f}(\mathbf{x}) + \sum_{i=1}^{2} \mathbf{g}_i(\mathbf{x})\mathrm{u}_i + \boldsymbol{\delta}(\cdot)$, where $\mathbf{x} = \begin{bmatrix}\boldsymbol{\eta}^\top & \boldsymbol{\nu_r}^\top\end{bmatrix}^\top = [x \;\; y \;\; \psi \;\; u_r \;\; v_r \;\; r]^\top$ is the state vector, $\mathbf{g}_i(\cdot)$ are the control vector fields and $\boldsymbol{\delta}(\cdot) = [V_c \cos\beta_c \;\; V_c \sin\beta_c \;\; \mathbf{0}_{1\times 4}]^\top$ is the perturbation vector field.
The dynamic nonholonomic constraint (27e) implies that $\mathbf{x_e} = \mathbf{0}$ is an equilibrium point of (27) if $v_r = 0$ and $u_r r = 0$. One gets out of the first condition that $v = v_c$. Given that the linear velocity v of the vehicle along the sway d.o.f. should be zero at the equilibrium, it follows that $v_c = 0 \Rightarrow V_c \sin(\beta_c - \psi_e) = 0 \Rightarrow V_c = 0$ or $\psi_e = \beta_c + \kappa\pi$, $\kappa \in \mathbb{Z}$. Thus, the desired orientation $\psi_e = 0$ can be an equilibrium of (27) if $V_c = 0$, which corresponds to the nominal case, or if $\beta_c = 0$, i.e. if the current is parallel to the x-axis of the global frame $\mathcal{G}$. In the general case that $\beta_c \neq 0$, the current serves as a non-vanishing perturbation at the equilibrium $\boldsymbol{\eta_e}$, and therefore the closed-loop trajectories of (27) can only be rendered ultimately bounded in a neighborhood of $\boldsymbol{\eta_e}$.
Thus, the control design for (27) reduces into addressing the *practical* stabilization problem, i.e. to find state feedback control laws so that the system trajectories $\boldsymbol{\eta}(t)$ remain bounded around the desired configuration $\boldsymbol{\eta_d}$.
Following the control design ideas used in the nominal case, the system (27) is divided into two subsystems Σ_1, Σ_2, where Σ_1 consists of the kinematic equations (27a)-(27c) and the sway dynamics (27e), while the dynamic equations (27d), (27f) constitute the subsystem Σ_2. The velocities u_r, r are considered as virtual control inputs for the subsystem Σ_1, while the actual control inputs τ_u, τ_r are used to control the subsystem Σ_2.
Theorem 3 The trajectories $\boldsymbol{r}(t) = [x(t) \;\; y(t)]^\top$ of the subsystem Σ_1 approach the ball $\mathcal{B}(\boldsymbol{r_d}, r_b)$, while the trajectories $\psi(t)$ globally converge to the equilibrium $\psi_e = \beta_c + \kappa\pi$, $\kappa \in \mathbb{Z}$, under the control law $u_r = \gamma_1(\cdot)$, $r = \gamma_2(\cdot)$ given as:

$$\gamma_1(\cdot) = -k_1 \operatorname{sgn}\left(\boldsymbol{r_1}^\top \begin{bmatrix}\cos\psi \\ \sin\psi\end{bmatrix}\right) \tanh\left(\mu \|\boldsymbol{r_1}\|\right), \tag{28a}$$

$$\gamma_2(\cdot) = -k_2(\psi - \phi) + \dot{\phi}, \tag{28b}$$

where r_b is the ultimate bound given by (C.4). The proof is given in the Appendix C.
Remark 1 Recall that the evolution of the trajectories $\boldsymbol{\eta}(t)$ should respect the viability constraints, for the sensor system to be effective. Thus the vehicle is restricted to move on the left hyperplane w.r.t. the global y_G axis (Fig. 10), while its orientation $\psi(t)$ should (roughly) be in $[-\frac{\pi}{2}, \frac{\pi}{2}]$, so that the vehicle faces the target. Consider the case in Fig. 10, where $\boldsymbol{r_1}^\top \boldsymbol{r_d} > 0$: the vehicle enters the ball $\mathcal{B}(\boldsymbol{r_d}, r_0)$ under (28a) with linear relative velocity $u_r > 0$, $\boldsymbol{r_1}^\top \begin{bmatrix}\cos\psi \\ \sin\psi\end{bmatrix} < 0$. It was shown in the

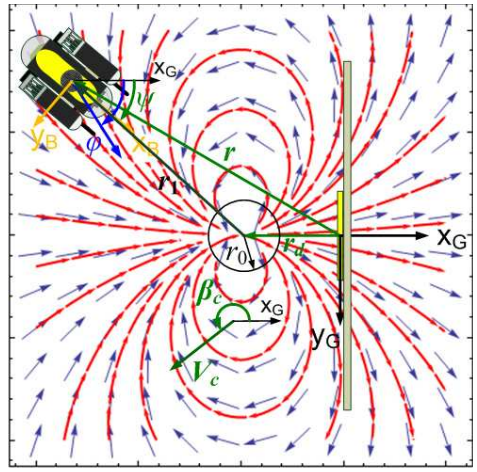

Fig. 10. The marine vehicle is controlled so that it aligns with the direction ϕ and flows along the integral curves of the vector field $\mathbf{F}(\cdot)$, until its trajectories $\boldsymbol{r}(t)$ remain bounded into a ball $\mathcal{B}(\boldsymbol{r_d}, r_0)$ and approach the ball $\mathcal{B}(\boldsymbol{r_d}, r_b)$.

Appendix C that after entering the ball $\mathcal{B}(\boldsymbol{r_d}, r_0)$, the vehicle converges to the equilibrium $\boldsymbol{\eta_e}$, where the linear velocity of the vehicle is $u = 0$, yielding $u_r = -u_c = -V_c \cos(\beta_c - \psi_e)$. The control input u_r given by (28a) at the equilibrium should be > 0 as well; otherwise one has out of (28a) that $\boldsymbol{r_1}^\top \begin{bmatrix}\cos\psi_e \\ \sin\psi_e\end{bmatrix} > 0$, i.e. that the vehicle does not face towards the target, which is undesirable. Then, it follows that $\cos(\beta_c - \psi_e) < 0$. Given that $\psi_e = \beta_c + \kappa\pi$, this further reads: $\cos(\beta_c - \psi_e) = -1 \Rightarrow \cos(\beta_c - \psi_e) = \cos\pi \Rightarrow \psi_e = \beta_c - \pi$. Then, in order to have $\psi_e \in [-\frac{\pi}{2}, \frac{\pi}{2}]$, so that the vehicle faces the target, it follows that $\beta_c \in [\frac{\pi}{2}, \frac{3\pi}{2}]$, i.e. that $\boldsymbol{r_1}^\top [\cos\beta_c \;\; \sin\beta_c] > 0$.
Remark 2 In the remaining of the paper we consider the class of bounded perturbations

$$\boldsymbol{\delta} = [V_c \cos\beta_c \;\; V_c \sin\beta_c \;\; \mathbf{0}_{1\times 4}], \quad \|\boldsymbol{\delta}\| \leq \|\boldsymbol{\delta}\|_{\max},$$

such that $\boldsymbol{r_1}^\top [\cos\beta_c \;\; \sin\beta_c] > 0$, see Fig. 10.
Theorem 4 The actual velocities $u_r(t)$, $r(t)$ are GES to the virtual control inputs $\gamma_1(\cdot)$, $\gamma_2(\cdot)$, respectively, under the control laws $\tau_u = \xi_1(\cdot)$, $\tau_r = \xi_2(\cdot)$ given as

$$\tau_u = m_{11}\alpha - m_{22} v_r r - X_u u_r - X_{u|u|}|u_r|u_r, \tag{29a}$$

$$\tau_r = m_{33}\beta - (m_{11} - m_{22}) u_r r - N_r r - N_{r|r|}|r|r \tag{29b}$$

where

$$\alpha = -k_u(u_r - \gamma_1(\cdot)) + (\nabla\gamma_1)\dot{\boldsymbol{\eta}}, \quad k_u > 0, \tag{30a}$$

$$\beta = -k_r(r - \gamma_2(\cdot)) + (\nabla\gamma_2)\dot{\boldsymbol{\eta}}, \quad k_r > 0. \tag{30b}$$

The proof is given in the Appendix D.

6.2 *Viable controls in the set K*

Assume that the vehicle is at a configuration $\boldsymbol{z} \in \mathcal{Z}_j$ where $\mathcal{Z}_j = \{\boldsymbol{z} \in \partial K \mid c_j(\cdot) = 0\}$, i.e. that j-th constraint becomes active. The map of viable controls at $\boldsymbol{z} \in \mathcal{Z}_j$ is given as $R_K(\boldsymbol{z}) := \{\boldsymbol{\tau} \in \mathcal{T}(\boldsymbol{z}) \mid \nabla c_j(\cdot)\, \dot{\boldsymbol{\eta}} \leq 0\}$, where $\nabla c_j(\cdot) = \left[\frac{\partial c_j}{\partial x} \ \frac{\partial c_j}{\partial y} \ \frac{\partial c_j}{\partial \psi}\right]^\top$ is the gradient of $c_j(\boldsymbol{\eta})$. Thus, the necessary conditions for selecting viable controls when the j-th constraint becomes active are analytically written as:

$$\nabla c_1 \dot{\boldsymbol{\eta}} \le 0 \Rightarrow \left[-\tan(\psi-\alpha) \ \ 1 \ \ -x\sec^2(\psi-\alpha)\right]\dot{\boldsymbol{\eta}} \le 0 \overset{(27)}{\Rightarrow}$$
$$(-\tan(\psi-\alpha)\cos\psi+\sin\psi)\,u_r - x\sec^2(\psi-\alpha)r$$
$$+\,(\tan(\psi-\alpha)\sin\psi+\cos\psi)\,v_r - \tan(\psi-\alpha)V_c\cos\beta_c$$
$$+\,V_c\sin\beta_c \le 0, \tag{31a}$$

$$\nabla c_2 \dot{\boldsymbol{\eta}} \le 0 \Rightarrow \left[\tan(\psi+\alpha) \ \ -1 \ \ x\sec^2(\psi+\alpha)\right]\dot{\boldsymbol{\eta}} \le 0 \overset{(27)}{\Rightarrow}$$
$$(\tan(\psi+\alpha)\cos\psi-\sin\psi)\,u_r + x\sec^2(\psi+\alpha)r$$
$$-\,(\tan(\psi+\alpha)\sin\psi+\cos\psi)\,v_r + \tan(\psi+\alpha)V_c\cos\beta_c$$
$$-\,V_c\sin\beta_c \le 0, \tag{31b}$$

$$\nabla c_3 \dot{\boldsymbol{\eta}} \le 0 \Rightarrow [\sec\psi \ \ 0 \ \ x]\,\dot{\boldsymbol{\eta}} \le 0 \overset{(27)}{\Rightarrow}$$
$$u_r + x\,r - \tan\psi\ v_r + \sec\psi V_c\cos\beta_c \le 0, \tag{31c}$$

$$\nabla c_4 \dot{\boldsymbol{\eta}} \le 0 \Rightarrow [-\sec\psi \ \ 0 \ \ -x]\,\dot{\boldsymbol{\eta}} \le 0 \overset{(27)}{\Rightarrow}$$
$$\tan\psi\ v_r - u_r - x\,r - \sec\psi V_c\cos\beta_c \le 0. \tag{31d}$$

Given that the velocities u_r, r serve as the control inputs, one should check whether the convergent control law (28) satisfies the viability conditions (31) at $\boldsymbol{z} \in \mathcal{Z}_j$. If this is not the case, then the control law should be re-designed so that the viability conditions are met at $\boldsymbol{z} \in \mathcal{Z}_j$. Clearly, if more than one constraints become active at the same time at some $\boldsymbol{z} \in \bigcap_{j\in\mathcal{J}} \mathcal{Z}_j$, the corresponding conditions should hold at the same time.

The conditions (31) offer the way to select viable control inputs at $\boldsymbol{z} \in \mathcal{Z}_j$. Consider, for instance, that $\boldsymbol{z} \in \mathcal{Z}_1$, which corresponds to the target being adjacent to the left boundary of the f.o.v.; then one can choose to regulate the orientation ψ to the angle $\phi_t = \text{atan2}(-y,-x)$ via the angular velocity $r_{viab_1} = -k(\psi - \phi_t)$, as one did for the nominal case. In this way, the vehicle is controlled so that target is centered in the camera f.o.v.. To select the gain k in a robust, yet conservative, way one can resort to picking k so that the resulting r_{viab_1} dominates the *worst-case* remaining terms in (21), i.e. the worst-case terms involving the upper bounds $|u_r|$, v_{r_b}, $\|\boldsymbol{\delta}\|$. Similarly, if $\boldsymbol{z} \in \mathcal{Z}_2$, i.e. if the target is adjacent to the right boundary of the f.o.v., the system can be as well controlled so that the target is centered in the camera f.o.v., via $r_{viab_2} = -k(\psi - \phi_t)$. In the same spirit, for the remaining constraints and for the class of perturbations considered in this paper (see the previous section) one can verify that by setting $r_{viab_{3,4}} = 0$ and $u_{r,viab_{3,4}}$ by (28a), where $k_1 \ge V_c$, the term involving u_r is negative and dominates the worst-case term involving V_c, implying that viability is maintained.

Therefore, for redesigning the control laws (28a), (28b) so that they are viable at $\boldsymbol{z} \in \mathcal{Z}_j$ one can consider the continuous switch (23) and use the control law

$$u_r = \sigma_j(c_j)u_{r,conv} + (1-\sigma_j(c_j))u_{r,viab_j}, \tag{32a}$$

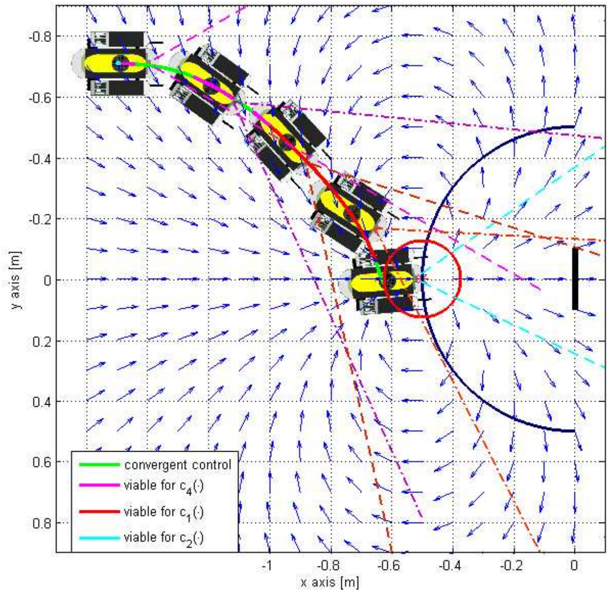

Fig. 11. The switching signal

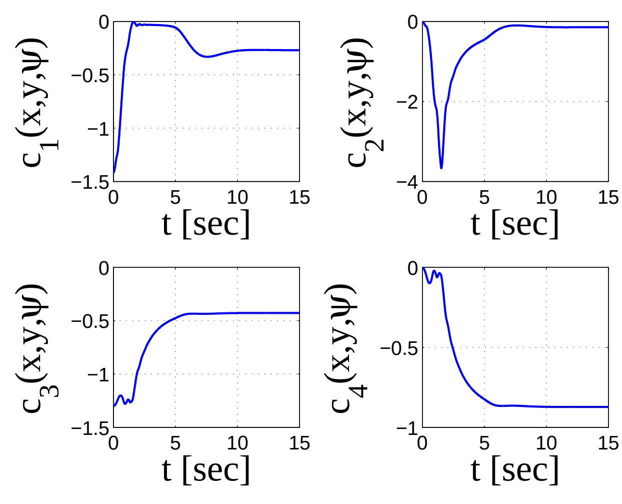

Fig. 12. The switching signal

$$r = \sigma_j(c_j)r_{conv} + (1-\sigma_j(c_j))r_{viab_j}, \tag{32b}$$

where $u_{r,conv}$, r_{conv} are given by (28), and $u_{r,viab_j}$, r_{viab_j} are control inputs satisfying the corresponding condition out of (22) at $\boldsymbol{z} \in \mathcal{Z}_j$. The orchestration of the switching between convergent and viable control laws taking into consideration all j constraints can be implemented similarly to the nominal case, by replacing the switching signal $\sigma_j(c_j)$ with $\sigma^* = \min(\sigma_j)$, $j \in \mathcal{J}$:

$$u_r = \min(\sigma_j)u_{r,conv} + (1-\min(\sigma_j))u_{r,viab_j}, \tag{33a}$$
$$r = \min(\sigma_j)r_{conv} + (1-\min(\sigma_j))r_{viab_j}, \tag{33b}$$

so that the system switches when necessary to the viable controls $u_{r,viab_j}$, r_{viab_j} that correspond to the constraint j which is closer to be violated.

In the case that the control laws $u_{r,viab}$, r_{viab} are not

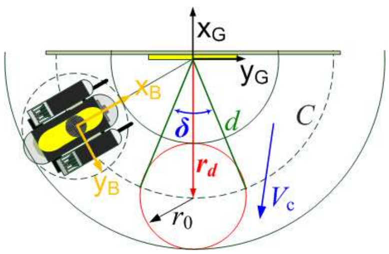

Fig. 13. The vehicle is forced to converge into a goal set $G \subset K$, defined as the union of the balls $\mathcal{B}(\boldsymbol{r_d}, r_0)$, where $\boldsymbol{r_d}$ belong to the circle C.

convergent into the ball $\mathcal{B}(\boldsymbol{r_d}, r_0)$, the switching control law (32) does not any longer guarantee the convergence of the system trajectories $\boldsymbol{r}(t)$ into $\mathcal{B}(\boldsymbol{r_d}, r_0)$. In this case, one can relax the requirement on the convergence into $\mathcal{B}(\boldsymbol{r_d}, r_0)$ where $\boldsymbol{r_d}$ a single point, and rather consider a set $C \subset K$ of desired configurations as

$$C = \left\{ \boldsymbol{\eta_d} \in K \mid {x_d}^2 + {y_d}^2 = d^2, \psi_d = \operatorname{atan2}(-y_d, -x_d) \right\},$$

where d is the desired distance w.r.t. the target, which define a circle of center $(x, y) = (0, 0)$ and radius d. Then, the vehicle can be controlled to converge into the set G, defined as the union of the balls $\mathcal{B}(\boldsymbol{r_d}, r_0)$, $\boldsymbol{r_d} \in C$ (Fig. 13). To do so, the viable velocities in (32) are chosen as

$$u_{r,viab} = -k_1 \operatorname{sgn}\left(\boldsymbol{r_1}^\top \begin{bmatrix} \cos\psi \\ \sin\psi \end{bmatrix} \right) \tanh(\mu \|\boldsymbol{r_1}\|), \quad (34a)$$

$$r_{viab} = -k(\psi - \phi_t), \quad (34b)$$

where $\phi_t = \operatorname{atan2}(-y, -x)$, $x_1 = x - x_d$, $x_d = d\cos\psi_d$, $y_1 = y - y_d$, $y_d = d\sin\psi_d$. Following the analysis in the previous sections, one has that the vehicle approaches the ball of radius $r_b = \frac{1}{\mu} \operatorname{artanh}\left(\frac{\|\boldsymbol{\delta}\|_{\max}}{k_1} \right)$ around some $\boldsymbol{r_d} \in C$. If the current direction β_c belongs into the cone of angle δ shown in Fig. 13, then the vehicle converges into the “nominal” ball $\mathcal{B}(\boldsymbol{r_d}, r_0)$, shown in red.
Finally, the control gains k_1, k_2, k_u, k_r can be properly tuned so that the “virtual” control inputs u_r, r correspond to thrust forces F_p, F_{st} that belong into the compact set $\mathcal{U} = [-f_p, f_p] \times [-f_{st}, f_{st}]$.

7 Conclusions

This paper presented a method for the feedback control design of nonholonomic systems which are subject to state constraints defining a viability set K. Using concepts from viability theory, the necessary conditions for selecting viable control laws for a nonholonomic system were given. Furthermore, a class of nonholonomic control solutions were redesigned in a switching control scheme, so that system trajectories starting in K converge to a goal set G in K, without ever leaving K. As a case study, the control design for an underactuated marine vehicle subject to configuration constraints due to limited visibility, as well as to a class of bounded external disturbances, was treated. Viable state feedback control laws in the constrained set K, which furthermore establish convergence to a goal set $G \subset K$ were constructed. Our plans for future extensions include the consideration of a wider class of external perturbations.

References

[1] W. E. Dixon, D. M. Dawson, E. Zergeroglu, A. Behal, Robustness to kinematic disturbances, in: Nonlinear Control of Wheeled Mobile Robots, Vol. 262 of Lecture Notes in Control and Information Sciences, Springer Berlin / Heidelberg, 2001, pp. 113–130.

[2] D. A. Lizarraga, N. P. I. Aneke, H. Nijmeijer, Robust point stabilization of underactuated mechanical systems via the extended chained form, SIAM Journal on Control and Optimization 42 (6) (2003) 2172–2199.

[3] C. Prieur, A. Astolfi, Robust stabilization of chained systems via hybrid control, IEEE Transactions on Automatic Control 48 (10) (2003) 1768–1772.

[4] Y. Guo, Nonlinear H_∞ control of uncertain nonholonomic systems in chained forms, International Journal of Intelligent Control and Systems 10 (4) (2005) 304–309.

[5] S. S. Ge, J. Wang, T. H. Lee, G. Y. Zhou, Adaptive robust stabilization of dynamic nonholonomic chained systems, Journal of Robotic Systems 18 (3) (2001) 119–133.

[6] P. Lucibello, G. Oriolo, Robust stabilization via iterative state steering with an application to chained-form systems, Automatica 37 (2001) 71–79.

[7] P. Morin, C. Samson, Practical stabilization of driftless systems on Lie groups: The transverse function approach, IEEE Transactions on Automatic Control 48 (9) (2003) 1496–1508.

[8] T. Floquet, J.-P. Barbot, W. Perruquetti, Higher-order sliding mode stabilization for a class of nonholonomic perturbed systems, Automatica 39 (2003) 1077–1083.

[9] E. Valtolina, A. Astolfi, Local robust regulation of chained systems, Systems and Control Letters 49 (2003) 231–238.

[10] X. Zhu, G. Dong, Z. Cai, D. Hu, Robust simultaneous tracking and stabilization of wheeled mobile robots not satisfying nonholonomic constraint, Journal of Central South University of Technology 14 (4) (2007) 537–545.

[11] H. K. Khalil, Nonlinear Systems. 3rd Edition, Prentice-Hall Inc., 2002.

[12] D. Liberzon, E. D. Sontag, Y. Wang, Universal construction of feedback laws achieving ISS and integral-ISS disturbance attenuation, Systems and Control Letters 46 (2002) 111–127.

[13] H. G. Tanner, ISS properties of nonholonomic vehicles, Systems and Control Letters 53 (3-4) (2004) 229–235.

[14] D. S. Laila, A. Astolfi, Input-to-state stability for discrete-time time-varying systems with applications to robust stabilization of systems in power form, Automatica 41 (2005) 1891–1903.

[15] A. P. Aguiar, J. P. Hespanha, A. M. Pascoal, Switched seesaw control for the stabilization of underactuated vehicles, Automatica 43 (2007) 1997–2008.

[16] A. K. Das, R. Fierro, V. Kumar, J. P. Ostrowski, J. Spletzer, C. J. Taylor, A vision-based formation control framework, IEEE Transactions on Robotics and Automation 18 (5) (2002) 813–825.

[17] N. Cowan, O. Shakernia, R. Vidal, S. Sastry, Vision-based follow-the-leader, in: Proc. of the 2003 IEEE/RSJ Intl. Conference on Intelligent Robots and Systems, Las Vegas, Nevada, 2003, pp. 1796–1801.

[18] F. Morbidi, F. Bullo, D. Prattichizzo, Visibility maintenance via controlled invariance for leader-follower vehicle formations, Automatica 47 (5) (2011) 1060–1067.

[19] D. Panagou, V. Kumar, Maintaining visibility for leader-follower formations in obstacle environments, in: Proc. of the 2012 International Conference on Robotics and Automation, St. Paul, Minnesota, USA, 2012, pp. 1811–1816.

[20] G. Kantor, A. A. Rizzi, Feedback control of underactuated systems via sequential composition: Visually guided control of a unicycle, in: P. Dario, R. Chatila (Eds.), Robotics Research, Springer Berlin Heidelberg, 2005, pp. 281–290.

[21] S. Bhattacharya, R. Murrieta-Cid, S. Hutchinson, Optimal paths for landmark-based navigation by differential-drive vehicles with field-of-view constraints, IEEE Transactions on Robotics 23 (1) (2007) 47–59.

[22] G. A. D. Lopes, D. E. Koditschek, Visual servoing for nonholonomically constrained three degree of freedom kinematic systems, International Journal of Robotics Research 26 (7) (2007) 715–736.

[23] J. Chen, D. M. Dawson, W. E. Dixon, V. K. Chitrakaran, Navigation function-based visual servo control, Automatica 43 (2007) 1165–1177.

[24] N. R. Gans, G. Hu, K. Nagarajan, W. E. Dixon, Keeping multiple moving targets in the field of view of a mobile camera, IEEE Transactions on Robotics 27 (4) (2011) 822–828.

[25] J. W. Durham, A. Franchi, F. Bullo, Distributed pursuit-evasion with limited-visibility sensors via frontier-based exploration, in: Proc. of the 2010 IEEE International Conference on Robotics and Automation, Anchorage, Alaska, 2010, pp. 3562–3568.

[26] F. Bullo, J. Cortés, S. Martínez, Distributed Control of Robotic Networks, Applied Mathematics Series, Princeton University Press, 2009, electronically available at http://coordinationbook.info.

[27] J.-P. Aubin, Viability Theory, Birkhäuser, 1991.

[28] D. Panagou, H. G. Tanner, K. J. Kyriakopoulos, Control of nonholonomic systems using reference vector fields, in: Proc. of the 50th IEEE Conference on Decision and Control and European Control Conference, Orlando, Florida, 2011, pp. 2831–2836.

[29] J.-P. Aubin, Viability kernels and capture basins of sets under differential inclusions, SIAM Journal on Control and Optimization 40 (3) (2001) 853–881.

[30] F. Blanchini, Set invariance in control, Automatica 35 (11) (1999) 1747–1767.

[31] F. Blanchini, S. Miani, Set-Theoretic Methods in Control, Birkhauser, 2008.

[32] N. E. Leonard, Periodic forcing, dynamics and control of underactuated spacecraft and underwater vehicles, in: Proc. of the 34th IEEE Conf. on Decision and Control, New Orleans, LA, USA, 1995, pp. 3980–3985.

[33] K. Y. Pettersen, O. Egeland, Time-varying exponential stabilization of the position and attitude of an underactuated Autonomous Underwater Vehicle, IEEE Trans. on Automatic Control 44 (1) (1999) 112–115.

[34] K. Y. Pettersen, T. I. Fossen, Underactuated dynamic positioning of a ship - Experimental results, IEEE Trans. on Control Systems Technology 8 (5) (2000) 856–863.

[35] T. I. Fossen, J. P. Strand, Nonlinear passive weather optimal positioning control (WOPC) system for ships and rigs: experimental results, Automatica 37 (2001) 701–715.

[36] A. P. Aguiar, A. M. Pascoal, Dynamic positioning of underactuated auv in the presence of a constant unknown ocean current disturbance, in: Proc. of the 15th IFAC World Congress, Barcelona, Spain, 2002.

[37] T. I. Fossen, M. Breivik, R. Skjetne, Line-of-sight path following of underactuated marine craft, in: Proc. of the IFAC MCMC'03, Girona, Spain, 2003.

[38] K. D. Do, Z. P. Jiang, J. Pan, H. Nijmeijer, A global output-feedback controller for stabilization and tracking of underactuated ODIN: A spherical underwater vehicle, IFAC Automatica 40 (2004) 117–124.

[39] D. Panagou, K. Margellos, S. Summers, J. Lygeros, K. J. Kyriakopoulos, A viability approach for the stabilization of an underactuated underwater vehicle in the presence of current disturbances, in: Proc. of the 48th IEEE Conference on Decision and Control, Shanghai, P.R. China, 2009, pp. 8612–8617.

[40] D. Panagou, K. J. Kyriakopoulos, Control of underactuated systems with viability constraints, in: Proc. of the 50th IEEE Conference on Decision and Control and European Control Conference, Orlando, Florida, 2011, pp. 5497–5502.

[41] M. Henle, A Combinatorial Introduction to Topology, Dover Publications, 1994.

[42] D. Shevitz, B. Paden, Lyapunov stability theory of nonsmooth systems, in: Proc. of the 32nd IEEE Conference on Decision and Control, San Antonio, Texas, USA, 1993, pp. 416–421.

[43] J.-P. Aubin, H. Frankowska, Set-valued Analysis, Birkhäuser, 1990.

[44] A. Isidori, Nonlinear Control Systems. Third Edition, Springer, 1995.

[45] T. I. Fossen, Marine Control Systems: Guidance, Navigation and Control of Ships, Rigs and Underwater Vehicles, Marine Cybernetics, 2002.

A Proof of Theorem 1

Proof Let us first prove the following lemma:

Lemma 1 *The orientation error* $e = \psi - \phi$ *is GES to zero under the control law* (17b).

Proof Take the positive definite, radially unbounded function $V_e = \frac{1}{2}e^2$, then its time derivative reads $\dot{V}_e = e\,\dot{e} \overset{(13c)}{=} (\psi - \phi)(r - \dot{\phi}) \overset{(17b)}{=} -k_2(\psi-\phi)^2 = -2k_2 V_e$. □

In order to study the convergence of the trajectories $\boldsymbol{\eta}(t)$ to $\boldsymbol{\eta_d}$, one can take a function V in terms of the position errors $x_1 = x - x_d$, $y_1 = y - y_d$ and the orientation error $e = \psi - \phi$ as $V = \frac{1}{2}({x_1}^2 + {y_1}^2) + \frac{1}{2}e^2 = V_1 + \frac{1}{2}e^2$, which is positive definite w.r.t. $[x_1 \;\; y_1 \;\; e]^\top$ and radially unbounded, and take its time derivative as

$$\dot{V} = \dot{V}_1 + e\,\dot{e} \overset{(13),(17b)}{=} -k_2 e^2 + \\ + [x_1 \;\; y_1] \begin{bmatrix} \cos\psi \\ \sin\psi \end{bmatrix} u + [x_1 \;\; y_1] \begin{bmatrix} -\sin\psi \\ \cos\psi \end{bmatrix} v. \qquad \text{(A.1)}$$

The behavior of $\dot{V}$ depends on the velocity v. If v can be seen as a bounded perturbation that vanishes at $[x_1 \;\; y_1 \;\; e]^\top = \mathbf{0}$, then this point is an equilibrium of the kinematic subsystem and therefore it is meaningful to analyze its (asymptotic) stability.

Since v comes from the control input $\zeta = ur$, one should study its evolution in an ISS framework. With this insight, consider the candidate ISS-Lyapunov function $V_v = \frac{1}{2}v^2$ and take its time derivative $\dot{V}_v = -\frac{m_{11}}{m_{22}}v(ur) - \left(\frac{|Y_v|}{m_{22}}v^2 + \frac{|Y_{v|v|}|}{m_{22}}|v|\,v^2\right)$, where by definition $Y_v, Y_{v|v|} < 0$, and $w(v) = \frac{|Y_v|}{m_{22}}v^2 + \frac{|Y_{v|v|}|}{m_{22}}|v|\,v^2$ is a continuous, positive definite function. Take $0 < \theta < 1$, then $\dot{V}_v = -\frac{m_{11}}{m_{22}}v(ur) - (1-\theta)w(v) - \theta w(v) \Rightarrow$

$$\dot{V}_v \leq -(1-\theta)w(v),\ \forall v : -\frac{m_{11}}{m_{22}}v(ur) - \theta w(v) < 0.$$

If the control input $\zeta = ur$ is bounded, $|\zeta| \leq \zeta_b$, then

$$\dot{V}_v \leq -(1-\theta)w(v),\ \forall |v| : |Y_v||v| + |Y_{v|v|}||v|^2 > \frac{m_{11}}{\theta}\zeta_b.$$

Then, the subsystem (13e) is ISS [11, Thm 4.19]. Thus, for any bounded input $\zeta = ur$, the linear velocity $v(t)$ will be ultimately bounded by a class $\mathcal{K}$ function of $\sup_{t>0}|\zeta(t)|$. If furthermore $\zeta(t) = u(t)r(t)$ converges to zero as $t \to \infty$, then $v(t)$ converges to zero as well [11]. Consequently, if the control inputs $u = \gamma_1(\cdot)$, $r = \gamma_2(\cdot)$ are bounded functions which converge to zero as $t \to \infty$, then one has that $v(t)$ is bounded and furthermore, $v(t) \to 0$ as $t \to \infty$. Going back to (A.1), substituting $u = \gamma_1(x, y)$ by (17a) yields

$$\dot{V} = -k_1\left|[x_1\ \ y_1]\begin{bmatrix}\cos\psi\\ \sin\psi\end{bmatrix}\right|\tanh(\mu\|\boldsymbol{r_1}\|) - k_2e^2 + \\ + [x_1\ \ y_1]\begin{bmatrix}\cos(\frac{\pi}{2}-\psi)\\ \sin(\frac{\pi}{2}-\psi)\end{bmatrix}v(t) = \dot{V}_1 - k_2e^2,$$

The control input $u(t)$ is bounded. Furthermore, one has out of (17b) that the control input $r(t)$ is bounded as well, since e, $\dot{\phi}$ are bounded. Therefore $v(t)$ is bounded: $|v(t)| \leq v_b$. The derivative $\dot{V}$ then reads:

$$\dot{V} \leq -k_1\left|[x_1\ \ y_1]\begin{bmatrix}\cos\psi\\ \sin\psi\end{bmatrix}\right|\tanh(\mu\|\boldsymbol{r_1}\|) + \|\boldsymbol{r_1}\|v_b - k_2e^2.$$

Thus, a sufficient condition for $\dot{V}_1 \leq 0$ can be taken as

$$\|\boldsymbol{r_1}\|v_b \leq k_1\left|\boldsymbol{r_1}^\top\begin{bmatrix}\cos\psi\\ \sin\psi\end{bmatrix}\right|\tanh(\mu\|\boldsymbol{r_1}\|) \leq k_1\|\boldsymbol{r_1}\|\tanh(\mu\|\boldsymbol{r_1}\|) \Rightarrow$$
$$v_b \leq k_1\tanh(\mu\|\boldsymbol{r_1}\|) \Rightarrow \|\boldsymbol{r_1}\| \geq \frac{1}{\mu}\text{artanh}(\frac{v_b}{k_1}), \quad \text{(A.2)}$$

where artanh$(\cdot)$ is the inverse hyperbolic tangent function. This condition essentially expresses that $\dot{V}_1 \leq 0$ for any position vector $\boldsymbol{r_1} = [x_1\ \ y_1]^\top$ that satisfies (A.2). Consequently, for any initial position $\boldsymbol{r_1}(0)$ and for any $0 \leq r_0 \leq \|\boldsymbol{r_1}(0)\|$ that satisfies (A.2), $\dot{V}_1$ is negative in the set $\{\boldsymbol{r_1} \mid \frac{1}{2}{r_0}^2 \leq V_1(\|\boldsymbol{r_1}\|) \leq \frac{1}{2}\|\boldsymbol{r_1}(0)\|^2\}$, which verifies that the trajectories $\boldsymbol{r_1}(t)$ enter and remain bounded in the set $\{\boldsymbol{r_1} \mid V_1(\boldsymbol{r_1}) \leq \frac{1}{2}{r_0}^2\}$, i.e. that $\boldsymbol{r_1}(t)$ enters and remains into the ball $\mathcal{B}(\mathbf{0}, r_0)$; equivalently, the trajectories $\boldsymbol{r}(t)$ enter and remain into the ball $\mathcal{B}(\boldsymbol{r_d}, r_0)$.

Note also that within the ball $\mathcal{B}(\boldsymbol{r_d}, r_0)$ the solution $\boldsymbol{r}(t)$ is bounded and belongs into $\mathcal{B}(\boldsymbol{r_d}, r_0)$ $\forall t > t_1$. Then, it follows that its positive limit set L^+ is a non-empty, compact invariant set; furthermore, $\boldsymbol{r}(t)$ approaches L^+ as $t \to \infty$ [11, Lemma 4.1].

Lemma 2 *The trajectories $\psi(t)$ of Σ_1 globally converge to the equilibrium $\psi_e = 0$ under the control law* (17b).

Proof Consider the time derivative $\dot{V}_e = -k_2e^2 \leq 0$, and denote $\Omega = \{e \mid \dot{V}_e = 0\} \Rightarrow \Omega = \{e \mid \psi = \phi(x, y)\}$. Then, the trajectories $e(t)$ converge to the largest invariant set M included in Ω.

The control input $r = \gamma_2(\cdot)$ given by (17b) vanishes when $\dot{\phi} = 0$, given that the orientation error $e = \psi - \phi(x, y)$ is GES to zero.

The dynamics of $\phi = \arctan\left(\frac{\mathrm{F}_y}{\mathrm{F}_x}\right)$ is $\dot{\phi} = \frac{\partial\phi}{\partial x}(x, y)\dot{x} + \frac{\partial\phi}{\partial y}(x, y)\dot{y}$. One can verify out of the analytic expressions of $\frac{\partial\phi}{\partial x}$, $\frac{\partial\phi}{\partial y}$ that $\dot{\phi}$ vanishes at the set $\mathrm{M}_1 = \{\mathbf{x} \mid x_1 = y_1 = 0 \wedge \psi = \phi(x_1, y_1) = 0\}$, or at the set $\mathrm{M}_2 = \{\mathbf{x} \mid x_1 \neq 0 \wedge y_1 = 0 \wedge \dot{y} = 0\}$, or at the set $\mathrm{M}_3 = \{\mathbf{x} \mid y_1 \neq 0 \wedge x_1 = 0 \wedge \dot{x} = 0\}$. For angular velocity $r = 0$, the sets further read $\mathrm{M}_1 = \{\mathbf{x} \mid x_1 = y_1 = \psi = 0 \wedge u = v = 0\}$, $\mathrm{M}_2 = \{\mathbf{x} \mid x_1 \neq 0 \wedge y_1 = 0 \wedge \psi = 0 \wedge v = 0\}$, $\mathrm{M}_3 = \{\mathbf{x} \mid y_1 \neq 0 \wedge x_1 = 0 \wedge \psi = \pi \wedge u = 0\}$. However, if the system trajectories start on or enter the set M_3, one has $u = \gamma_1(\cdot) \neq 0$, which implies that the trajectories escape M_3. On the other hand, it is easy to verify that the sets M_1, M_2 are invariant w.r.t. the trajectories $\psi(t)$; the set M_1 corresponds to the trivial solution where $u = r = 0$, whereas M_2 corresponds to the vehicle moving along the x_G axis with $u \neq 0$, $r = 0$.

Thus, $\dot{\phi}$ vanishes at the set $(\mathrm{M}_1 \vee \mathrm{M}_2)$. Therefore, the largest invariant set M in Ω reduces to $(\mathrm{M}_1 \vee \mathrm{M}_2)$, where one has $\psi = 0$, since in any other case the control input (17b) yields $r \neq 0$, which implies that $\psi = \phi(x, y)$ does not identically stay in Ω. Consequently, the orientation trajectories $\psi(t)$ globally converge to $\psi_e = 0$. □

Going back to the evolution of the position trajectories $\boldsymbol{r}(t)$, note that, within the ball $\mathcal{B}(\boldsymbol{r_d}, r_0)$, the control input $\zeta = ur$ vanishes as $r \to 0$. According to the above analysis, the control input $r(t)$ converges to zero as $(\psi \to \phi(x, y)) \wedge (\psi \to 0)$. Since the dynamics of v are ISS, one has out of $\zeta(t) \to 0$ that $v(t) \to 0$ as well. Consequently, one gets out of (A.2) that the system trajectories $\boldsymbol{r}(t)$ approach the ball $\mathcal{B}(\boldsymbol{r_d}, r_b)$ of radius: $r_b = \frac{1}{\mu}\,\text{artanh}\left(\frac{v(t)}{k_1}\right)$, where r_b is the ultimate bound of the system, $r_b < r_0$. Clearly, as $v(t) \to 0$, one also gets that the ultimate bound $r_b \to 0$, i.e. that $\boldsymbol{r}(t) \to \boldsymbol{r_d}$. □

B Proof of Theorem 2

Proof Under the feedback linearization transformation (18) the dynamic subsystem (13d), (13f) reads $\dot{u} = \alpha$, $\dot{r} = \beta$, where α, β are the new control inputs. Consider the candidate Lyapunov function $V_\tau = \frac{1}{2}(u - \gamma_1(\boldsymbol{\eta}))^2 + \frac{1}{2}(r - \gamma_2(\boldsymbol{\eta}))^2$, and take its time derivative as $\dot{V}_\tau = (u - \gamma_1(\boldsymbol{\eta}))(\dot{u} - (\nabla\gamma_1)\dot{\boldsymbol{\eta}}) + (r - \gamma_2(\boldsymbol{\eta}))(\dot{r} - (\nabla\gamma_2)\dot{\boldsymbol{\eta}})$, where $\nabla\gamma_k = \left[\frac{\partial\gamma_k}{\partial x}\ \ \frac{\partial\gamma_k}{\partial y}\ \ \frac{\partial\gamma_k}{\partial\psi}\right]$,

$\mathtt{k} = 1, 2$. Under the control inputs (19) one gets

$$\dot{V}_\tau = -k_u(u-\gamma_1(\cdot))^2 - k_r(r-\gamma_2(\cdot))^2 \leq -2\min\{k_u, k_r\}V_\tau,$$

where $k_u, k_r > 0$, which verifies that the actual velocities u, r are GES to the virtual controls $\gamma_1(\cdot)$, $\gamma_2(\cdot)$, respectively. □

C Proof of Theorem 3

Proof The analysis on the trajectories of the perturbed system is along the same lines as the one for the nominal one. First, let us prove the following lemma:
Lemma 3 *The orientation error $e = \psi - \phi$ is GES to zero under the control law* (28b).
Proof Take the positive definite, radially unbounded function $V_e = \frac{1}{2}e^2$; then its time derivative reads $\dot{V}_e = e\dot{e} \overset{(27c)}{=} (\psi - \phi)(r - \dot{\phi}) \overset{(28b)}{=} -k_2(\psi - \phi)^2 = -2k_2 V_e$. □
To study the behavior of the system trajectories $\boldsymbol{r}(t)$ under (28), consider the Lyapunov function candidate

$$V_r = \frac{1}{2}\left((x - x_d)^2 + (y - y_d)^2\right) = \frac{1}{2}\left(x_1^2 + y_1^2\right), \quad \text{(C.1)}$$

which is positive definite, radially unbounded and of class C^∞, and take the derivative of V_r along the trajectories of (27), given that $\dot{x}_d = 0$, $\dot{y}_d = 0$:

$$\dot{V}_r = [x_1 \;\; y_1]\begin{bmatrix}\cos\psi \\ \sin\psi\end{bmatrix} u_r + [x_1 \;\; y_1]\begin{bmatrix}-\sin\psi \\ \cos\psi\end{bmatrix} v_r + \\ + [x_1 \;\; y_1]\begin{bmatrix}\cos\beta_c \\ \sin\beta_c\end{bmatrix} V_c. \quad \text{(C.2)}$$

The behavior of $\dot{V}_r$ depends on the linear velocity v_r along the sway d.o.f., as well as on the external perturbation. Since v_r comes from the control input $\zeta = u_r r$, one should study its evolution in an ISS framework. With this insight, consider the candidate ISS-Lyapunov function $V_v = \frac{1}{2}{v_r}^2$ and take its time derivative $\dot{V}_v = -\frac{m_{11}}{m_{22}}v_r(u_r r) - \left(\frac{|Y_v|}{m_{22}}{v_r}^2 + \frac{|Y_{v|v|}|}{m_{22}}|v_r|\,{v_r}^2\right)$;
following the same analysis as in the nominal case, and given that the control input ζ is bounded, $|\zeta| \leq \zeta_b$, one eventually gets for some $\theta \in (0, 1)$ that:

$$\dot{V}_v \leq -(1-\theta)w(v_r),\ \forall |v_r| : |Y_v||v_r| + |Y_{v|v|}||v_r|^2 \geq \frac{m_{11}}{\theta}\zeta_b.$$

Thus the subsystem (27e) is ISS w.r.t. ζ [11, Thm 4.19], which essentially expresses that for any bounded input $\zeta = u_r r$, the linear velocity $v_r(t)$ will be ultimately bounded by a class $\mathcal{K}$ function of $\sup_{t>0}|\zeta(t)|$. Furthermore, if $\zeta(t) = u_r(t)r(t)$ converges to zero as $t \to \infty$, then $v_r(t)$ converges to zero as well [11].
Remark 3 Note that the control input $\zeta(t)$ should vanish at the equilibrium $\boldsymbol{\eta_e} = [x_e \;\; y_e \;\; \psi_e]^\top$, which is dictated by the direction β_c of the external disturbance, since $\psi_e = \beta_c + \kappa\pi$, $\kappa \in \mathbb{Z}$. Nevertheless, assuming that the current V_c, β_c is known and constant is unrealistic; thus, knowing a priori the equilibrium $\boldsymbol{\eta_e}$ is in general infeasible. For this reason we assume that only the bound $\|\boldsymbol{\delta}\|_{\max}$ of the current velocity is known, while the direction β_c is arbitrary, so that

$$\|\boldsymbol{\delta}\| = \sqrt{(V_c\cos\beta_c)^2 + (V_c\sin\beta_c)^2} = |V_c| \leq \|\boldsymbol{\delta}\|_{\max}.$$

This practically means that the current disturbance can be of any, *not necessarily constant* direction β_c, as long as $|V_c| \leq \|\boldsymbol{\delta}\|_{\max}$.
Substituting the control law (28a) into (C.2) yields

$$\dot{V}_r = -k_1\left|\boldsymbol{r_1}^\top\begin{bmatrix}\cos\psi \\ \sin\psi\end{bmatrix}\right|\tanh\left(\mu\|\boldsymbol{r_1}\|\right) + [x_1 \;\; y_1]\begin{bmatrix}-\sin\psi \\ \cos\psi\end{bmatrix} v_r + \\ + [x_1 \;\; y_1]\begin{bmatrix}\cos\beta_c \\ \sin\beta_c\end{bmatrix} V_c \Rightarrow \\ \dot{V}_r \leq -k_1\left|\boldsymbol{r_1}^\top\begin{bmatrix}\cos\psi \\ \sin\psi\end{bmatrix}\right|\tanh\left(\mu\|\boldsymbol{r_1}\|\right) + \|\boldsymbol{r_1}\|\left(v_{rb} + \|\boldsymbol{\delta}\|_{\max}\right),$$

where v_{rb} is the ultimate bound of the linear velocity v_r. Thus, a sufficient condition for $\dot{V}_r < 0$ can be taken as

$$\|\boldsymbol{r_1}\|(v_{rb} + \|\boldsymbol{\delta}\|_{\max}) < k_1\left|\boldsymbol{r_1}^\mathrm{T}\begin{bmatrix}\cos\psi \\ \sin\psi\end{bmatrix}\right|\tanh\left(\mu\|\boldsymbol{r_1}\|\right) \leq \\ \leq k_1\|\boldsymbol{r_1}\|\tanh\left(\mu\|\boldsymbol{r_1}\|\right) \\ \Rightarrow v_{rb} + \|\boldsymbol{\delta}\|_{\max} < k_1\tanh\left(\mu\|\boldsymbol{r_1}\|\right) \\ \Rightarrow \|\boldsymbol{r_1}\| > \frac{1}{\mu}\operatorname{artanh}\left(\frac{v_{rb} + \|\boldsymbol{\delta}\|_{\max}}{k_1}\right), \quad \text{(C.3)}$$

where artanh$(\cdot)$ is the inverse hyperbolic tangent function. This condition essentially expresses that one has $\dot{V}_r < 0$ for any position vector $\boldsymbol{r_1} = [x_1 \;\; y_1]^\top$ that satisfies (C.3). Thus, for any initial position $\boldsymbol{r_1}(0)$ and for any $r_0 < \|\boldsymbol{r_1}(0)\|$ that satisfies (C.3), $\dot{V}_r$ is negative in the set $\{\boldsymbol{r_1} \mid \frac{1}{2}{r_0}^2 \leq V_r(\|\boldsymbol{r_1}\|) \leq \frac{1}{2}\|\boldsymbol{r_1}(0)\|^2\}$, which verifies that the trajectories $\boldsymbol{r}(t)$ enter and remain bounded into the ball $\mathcal{B}(\boldsymbol{r_d}, r_0)$.
Note also that within the ball $\mathcal{B}(\boldsymbol{r_d}, r_0)$ the solution $\boldsymbol{r}(t)$ is bounded and belongs into $\mathcal{B}(\boldsymbol{r_d}, r_0)$ $\forall t > t_1$. Then, it follows that its positive limit set L^+ is a non-empty, compact invariant set; furthermore, $\boldsymbol{r}(t)$ approaches L^+ as $t \to \infty$ [11, Lemma 4.1].
Lemma 4 *The trajectories $\psi(t)$ of the subsystem Σ_1 globally converge to the equilibrium $\psi_e = \beta_c \pm \pi$ under the control law* (28b).
Proof To verify the argument, consider the time derivative $\dot{V}_e = -k_2 e^2 \leq 0$ of the positive definite, radially unbounded function $V_e = \frac{1}{2}e^2$. Denote $\Omega = \{e \mid \dot{V}_e = 0\} \Rightarrow \Omega = \{e \mid \psi = \phi(x, y)\}$. Then, the trajectories $e(t)$ converge to the largest invariant set M included in Ω. Note that the control input (28b) vanishes when $\dot{\phi} = 0$, given that the tracking error $e = \psi - \phi(x, y)$ is GES to zero. Taking the dynamics of $\phi = \arctan(\frac{\mathrm{F}_y}{\mathrm{F}_x})$ yields that $\dot{\phi} = \mathrm{f}_1(x, y)\dot{x} + \mathrm{f}_2(x, y)\dot{y}$. The functions $\mathrm{f}_1(x, y)$, $\mathrm{f}_2(x, y)$ vanish only at $x = x_d$, $y = y_d$; nevertheless, it was shown that the system trajectories $\boldsymbol{r}(t)$ never reach

the desired position $\boldsymbol{r_d}$, unless the perturbation is vanishing. Thus, $\dot{\phi}$ vanishes only when $\dot{x} = \dot{y} = 0$, i.e. at the equilibrium of (27), at which the vehicle's orientation is $\psi_e = \beta_c \pm \pi$. Therefore, the largest invariant set M reduces to $\psi_e = \beta_c \pm \pi$, since if $\psi = \phi(x, y) \neq \psi_e$, the control input (28b) yields $r \neq 0$, which implies that ψ does not identically stay in Ω. □

Going back to the position trajectories $\boldsymbol{r}(t)$, one has that within the ball $\mathcal{B}(\boldsymbol{r_d}, r_0)$ the control input $\zeta(t) = u_r(t)\, r(t)$ vanishes as $r(t) \to 0$.[6] According to the above analysis, this occurs when $\psi = \phi(x, y)$ *and* $\psi = \beta_c \pm \pi$, i.e. when the orientation ψ of the vehicle is aligned with the direction of the current, at a point (x, y) where the reference orientation $\phi(x, y)$ coincides with the direction of the current as well; then out of (28b) one has $r = 0$. Since the dynamics of v_r are ISS, it follows that $\zeta(t) \to 0$ implies that $v_r(t) \to 0$. Consequently, one gets out of (C.3) that the system trajectories $\boldsymbol{r}(t)$ approach the ball $\mathcal{B}(\boldsymbol{r_d}, r_b)$ of radius $r_b < r_0$, given as:

$$r_b = \frac{1}{\mu} \operatorname{artanh}\left(\frac{\|\boldsymbol{\delta}\|_{\max}}{k_1}\right), \tag{C.4}$$

where r_b is the ultimate bound of the system. □

Note that the ultimate bound r_b depends on the norm of the perturbation $\|\boldsymbol{\delta}\|_{\max}$, as well as on the control gain k_1 on the linear velocity, as one would expect from physical intuition.

D Proof of Theorem 4

Proof Under the feedback linearization transformation (29) the corresponding dynamic equations (27d), (27f) read $\dot{u}_r = \alpha$, $\dot{r} = \beta$, respectively, where α, β are the new control inputs. Consider the candidate Lyapunov function $V_\tau = \frac{1}{2}\left(u_r - \gamma_1(\cdot)\right)^2 + \frac{1}{2}\left(r - \gamma_2(\cdot)\right)^2$, and take its time derivative as $\dot{V}_\tau = \left(u_r - \gamma_1(\cdot)\right)\left(\dot{u}_r - \frac{\partial \gamma_1}{\partial \boldsymbol{\eta}}\dot{\boldsymbol{\eta}}\right) + \left(r - \gamma_2(\cdot)\right)\left(\dot{r} - \frac{\partial \gamma_2}{\partial \boldsymbol{\eta}}\dot{\boldsymbol{\eta}}\right)$. Then, under the control inputs (30) one gets $\dot{V}_\tau = -k_u(u_r - \gamma_1(\cdot))^2 - k_r(r - \gamma_2(\cdot))^2 \leq -2\min\{k_u, k_r\}V_\tau$, which verifies that the actual velocities $u_r(t)$, $r(t)$ are globally exponentially stable to the virtual velocities $\gamma_1(\cdot)$, $\gamma_2(\cdot)$, respectively. □

[6] It is easy to verify that $u_r(t)$ given by (28a) never vanishes, since $\boldsymbol{r_1}(t)$ does not converge to zero.